Anselmetti, F.S., Isern, A.R., Blum, P., and Betzler, C. (Eds.)
Proceedings of the Ocean Drilling Program, Scientific Results Volume 194

5. Biosedimentary and Paleoenvironmental Evolution of the Southern Marion Platform from the Middle to Late Miocene (Northeast Australia, ODP Leg 194, Sites 1196 and 1199)[1]

Gilles A.R. Conesa,[2] Eric Favre,[3] Philippe Münch,[2]
Hélène Dalmasso,[2] and Christian Chaix[4]

ABSTRACT

The Southern Marion Plateau (SMP) represents a vertical stacking of Miocene carbonate platform deposits. Two sites (1196 and 1199) were drilled on top of this plateau, penetrating a 663-m carbonate succession of bioclastic and reefal sedimentary bodies. The study focuses on the least dolomitized 410-m-thick upper part of the succession, which is middle to late Miocene in age. Sedimentological and paleontological studies were conducted at both sites in order to propose a paleoenvironmental model and its evolution through the Miocene age. Six main microfacies of possible environmental significance were defined using statistical multivariate analyses, based on the recognition and point counting of 24 biogenic components. Depositional environment reconstructions are proposed as well as the biosedimentary and the environmental evolution regarding seismic architectures, stratigraphy, biosedimentology, and microfacies analysis. The SMP platform mainly results from a vertical stacking of lens-shaped bodies in homoclinal to distally steepened ramp settings.

[1]Conesa, G.A.R., Favre, E., Münch, P., Dalmasso, H., and Chaix, C., 2005. Biosedimentary and paleoenvironmental evolution of the Southern Marion Platform from the middle to late Miocene (northeast Australia, ODP Leg 194, Sites 1196 and 1199). *In* Anselmetti, F.S., Isern, A.R., Blum, P., and Betzler, C. (Eds.), *Proc. ODP, Sci. Results,* 194, 1–38 [Online]. Available from World Wide Web: <http://www-odp.tamu.edu/publications/194_SR/VOLUME/CHAPTERS/005.PDF>. [Cited YYYY-MM-DD]
[2]Université Aix-Marseille I, Centre de Sédimentologie-Paléontologie, Case 67, 3 place Victor Hugo, 13331 Marseille Cedex, France. Correspondence author: **gilles.conesa@up.univ-mrs.fr**
[3]Université de Lyon I, UMR 5125 PEPS–CNRS, Bâtiment GEODE, 2 rue Raphael Dubois, 69622 Villeurbanne Cedex, France.
[4]Museum d'Histoire Naturelle de Paris, Département Histoire de la Terre, Bâtiment de Paléontologie, CP 38, 8 rue Buffon, 75005 Paris, France.

Initial receipt: 7 July 2003
Acceptance: 7 December 2004
Web publication: 3 June 2005
Ms 194SR-005

INTRODUCTION

The facies and paleoenvironmental evolution of Miocene carbonate platforms from northeast Australia were mostly known through scattered exploration wells (see synthesis of Davies et al., 1989) and Ocean Drilling Program (ODP) Leg 133 drilling of the Queensland and North Marion Plateaus (Davies, McKenzie, Palmer-Julson, et al., 1991; Betzler and Chapronière, 1993; Brachert et al., 1993; Chapronière and Betzler, 1993; Isern et al., 1993; Martín and Braga, 1993; Martín et al., 1993; McKenzie and Davies, 1993; Betzler et al., 1993, 1995; Betzler, 1997). ODP Leg 194 drilling operations were performed on two new carbonate platforms located north and south of the Marion Plateau (Fig. **F1**). Some of the objectives were to achieve a better understanding of carbonate platform development in the region with respect to climate, sea level fluctuations, and paleoceanography and to calculate the second-order magnitude of the late middle Miocene (N12–N14) sea level fall (Shipboard Scientific Party, 2002a, 2002b).

The Southern Marion Platform (SMP) is an isolated platform of the Marion Plateau, which is a deeper extension of the Australian continental margin (Davies et al., 1989) (Fig. **F2**). Before Leg 194, the SMP was mainly known through seismic analyses. It was considered late Miocene in age and nucleated on the slope sediments of the Northern Marion Platform after the late middle Miocene sea level fall (Pigram et al., 1992; Pigram, 1993; Liu et al., 1998). The Shipboard Scientific Party (2002a, 2002b) provided new detailed information about the SMP. Through several seismic transects (Fig. **F1**), they found evidence of an asymmetrical pattern for the SMP architecture with an escarpment-like margin on the northwestern side and a thick package of prograding clinoforms on the southeastern margin (Fig. **F2**). During Leg 194 drilling, hemipelagic and periplatform deposits on both margins were recovered from Sites 1197 and 1198 (~665 m thick and ~515 m thick, respectively), whereas a ~660-m-thick succession of shallow-water carbonates on top of the platform (Figs. **F1, F2, F3**) was penetrated at Sites 1196 and 1199. Underlying acoustic basement was reached and consists of either highly altered basalts (Sites 1197 and 1198) or phosphate-rich sands (Site 1196). The whole deposits were addressed to the seismic regional megasequences (A–D) of Pigram (1993), separated by sequence boundaries (Fig. **F2**). Megasequences B and C, both Miocene in age, contain the SMP (Fig. **F2**). In the Marion Plateau, the Megasequence B/C and C/D boundaries were further dated through seismic correlation to ~11.0 Ma and ~7.2 Ma, respectively (Shipboard Scientific Party, 2002a). The platform deposits were subdivided into four lithostratigraphic units at Sites 1196 and 1199. Site 1196 is situated 20 km east of the Great Barrier Reef at 304.2 meters below sea level (mbsl) and Site 1199 is situated 5 km northeast of Site 1196 at 315.9 mbsl (Fig. **F1**). Both sites were dated from early Miocene to Pliocene based on the determination of large benthic foraminifers, planktonic foraminifers, and calcareous nannofossils. The substrate was defined as a fifth lithostratigraphic unit, most likely latest Oligocene in age. At least three phases of growth, exposure, and dolomitization were recognized within the platform and partly correlated to the megasequences of Pigram (1993) (Fig. **F3**). The oldest phase is mostly early Miocene in age and is represented by a ~250-m-thick succession of dolostones with rhodoliths and corals preserved as ghosts (Units III–IV). The two youngest phases are early(?) to middle Miocene and most likely late Miocene in age, respectively,

F1. Location of Leg 194 and Leg 133 sites, p. 24.

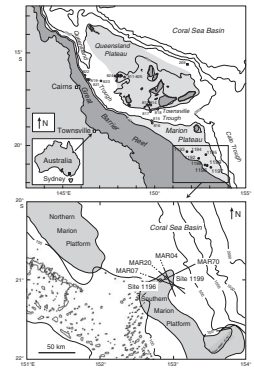

F2. Seismic transect of the SMP, p. 25.

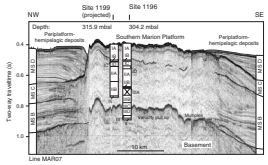

F3. Lithostratigraphy and architecture of the SMP, p. 26.

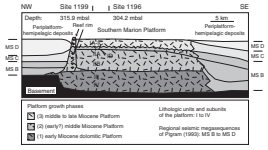

and consist of ~410-m-thick interbedded rhodalgal, coral, and porcellaneous foraminiferal (dolomitic) limestones (Units I–II). During the last two phases, the SMP was interpreted as asymmetrical with a flat-topped, reef-rimmed western margin and an eastern margin evolving from a distally steepened to a more homoclinal ramp (Shipboard Scientific Party, 2002a) (Figs. F2, F3) The lithologic boundary between the last two phases was ascribed to a surface exposure observed at the top of Subunit ID at Sites 1196 and 1199 (Fig. F3). A low-amplitude, low-frequency reflection at ~110–130 meters below seafloor (mbsf) underneath the top of the SMP was considered the corresponding seismic boundary. The reflection was correlated to the Megasequence B/C seismic boundary and partly related to the late middle Miocene (N12–N14) sea level fall (Fig. F2). The top of the platform is marked both by an exposure surface and by an overlying hardground surface a few centimeters thick. The hardground surface is represented by planktonic wackestone deposits and infillings dated to Pliocene with a maximum age of 3.2 Ma and by laminated ferromanganese crust (Shipboard Scientific Party 2002a, 2002b). It is assumed that the end of the youngest platform growth phase coincides with the Megasequence C/D seismic boundary and the drowning of the SMP (Fig. F3).

Our study focuses on the two youngest platform growth phases of the SMP and concerns the 410-m-thick upper part of the platform drilled at Sites 1196 (Holes 1196A and 1196B) and 1199. This part of the platform is the least dolomitized of the whole succession and is middle (early?) to late Miocene in age (Shipboard Scientific Party, 2002a). The aim of this study is

1. To define and describe microfacies of environmental significance through statistical multivariate analysis of biogenic components,
2. To determine and visualize the depositional environments with respect to the SMP's geometry and biosedimentology, and
3. To establish a link between the microfacies and environmental evolution of the platform and sea level fluctuations.

METHODOLOGY

Biosedimentological data from the studied platform succession were examined from the cores of both Holes 1196A and 1199A, using the onboard visual core descriptions (Shipboard Scientific Party, 2002b). Microfacies analysis with additional multivariate analysis of bioclasts was conducted on 84 thin sections originating from Holes 1196A, 1196B, and 1199A. A total of 24 categories of bioclasts were examined, including invertebrates, coralline algae, and foraminifers. Conventions from Coleman (1963), Adams (1968), Loeblich and Tappan (1988), Betzler and Chapronière (1993), Chapronière and Betzler (1993), and Boudagher-Fadel et al. (2000a, 2000b) were used for large benthic foraminifer determination, generally at a generic scale. Coral taxa and their ecological significance were determined following conventions from Beauvais et al., (1993), Boichart et al., (1985), Cahuzac and Chaix (1996), Chaix et al., (1986), Ditlev (1980), Vaughan and Wells (1943), Veron (2000), and Wells (1956). The coral assemblages are shown in Table T1. ADE-4 statistical programs from the University of Lyon I were used to analyze the data. A total of 59 thin sections with sufficient bioclasts were point-counted with at least 300 counts using a conventional grain solid tech-

T1. Coral taxa with ecological significance, Sites 1196 and 1199, p. 36.

nique. The quantitative values were entered into a contingency data matrix with thin sections in rows and categories of bioclasts in columns. These values were transformed to percentages and then ranked in value ranging from 0 to 9, using the logarithmic formula

$$\log_2(3X + 1),$$

where X = percentage. The transformation reduces large discrepancies between quantitative values. It allows multivariate analysis to take variables into account that have low values but possible high environmental significance (see Sokal and Rohlf, 2003, for more details). The obtained encoded data matrix was treated by ascendant cluster analysis (ACA) and by correspondence factor analysis (CFA).

The ACA permits ordering thin sections within groups of both increasing hierarchy and decreasing correlation, according to biological variables. Relationships between thin sections and groups are evaluated on a dendrogram. These groups are believed to represent microfacies. This microfacies matrix is obtained from the percentage matrix by rearrangement of rows, according to ACA ordination. The microfacies and the percentage of the biological variables are shown with lithostratigraphic units in Figure **F4.**

The CFA simultaneously computes correlations within and between thin sections and variables. It represents, within a multidimensional space of N factorial axis, the structure of data as two clouds of $N + 1$ variable points and M thin section points, respectively ($M > N$). The CFA runs an ordination of axes from 1 to N, according to the decrease of variance or inertia of both clouds. Complex relationships between thin sections and/or variables and their distribution were examined on factorial planes defined by the first axes, which collect most of the variance. Each variable and each thin section provide an absolute contribution (AC, part of variance) and a relative contribution (RC = $10{,}000 \times r^2$, where r = coefficient of correlation) to each axis. Only discriminative variables (AC > $10{,}000/N+1$ and RC > 2500, i.e., $|r| > 0.5$) were examined (see Benzécri et al., 1980, and Etter, 1999, for more details). The variables are given in Table **T2.**

The application of both ACA and CFA on the same encoded matrix allows the definition of microfacies that possibly contain specific environmental significance. Moreover, the application of both ACA and CFA allows us to define and explain the interrelationships between the microfacies regarding environmental trends (i.e., Cugny and Rey, 1981; Hennebert and Lees, 1991; Nebelsick, 1992). The statistical results are then used to develop three-dimensional depositional reconstructions that take into account information about seismic profiles, lithostratigraphy, biosedimentology, and microfacies analysis.

AGE AND LITHOSTRATIGRAPHY

In the studied vertical succession of the SMP, the same lithostratigraphic Units I (Subunits IA–ID) and II (Subunits IIA and IIB) were recognized at both Sites 1196 and 1199 by the Shipboard Scientific Party (2002a, 2002b) as well as Subunit IIIA at Site 1196 (Fig. **F5**). The total recovery at Site 1196 shows low percentages (Hole 1196A: Unit I = 13%, Unit 2 = 6.3%, Subunit IIIA = 1.5%; Hole 1196B: Unit I = 15.4%, Unit II = 4.5%) At Site 1199, the percentages are higher in Unit I (52.3%) and on the same order in Unit II (3.3%) with no recovery in Cores 194-

F4. Microfacies matrix with bioclast values and ACA dendrogram, p. 27.

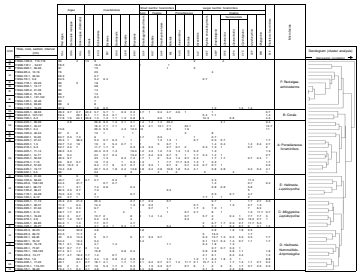

T2. CFA summary, p. 37.

F5. Biosedimentological data, microfacies, and environment evolution, p. 28.

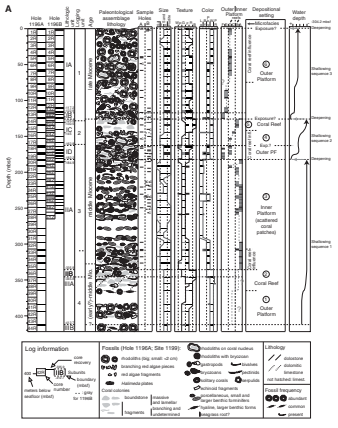

1199A-22R through 29R (Fig. F5). The Shipboard Scientific Party (2002a, 2002b) correlated the two sites in a schematic diagram representing the lithostratigraphy and the architecture of the SMP (Fig. F3). This lithostratigraphic framework is based on seismic architecture (Fig. F2), facies similarities, biostratigraphy, and some noticeable subunit boundaries interpreted as possible regional surface exposures or hardgrounds (Shipboard Scientific Party 2002a, 2002b). The onboard logging stratigraphy proposed a slightly different correlation pattern based on uranium contents and resistivity of the rocks (Fig. F6). The main difference between the lithostratigraphy and the logging stratigraphy concerns the correlation of Subunit IIB between the two sites.

Unit I was dated middle to late Miocene in age by the occurrence of *Lepidocyclina* spp. and planktonic foraminifers of Pliocene age at the top of the SMP (Shipboard Scientific Party, 2002b). Furthermore, Subunit IIA was dated middle Miocene in age using *Flosculinella bontangensis*, whereas Subunit IIB was dated early to middle Miocene in age by calcareous nannofossils found in the last core of Hole 1196A (Shipboard Scientific Party, 2002b). Using the most recent foraminifer biostratigraphy of the Indo-Pacific (Boudagher-Fadel and Banner, 1999; Boudagher-Fadel et al., 2000a, 2000b), we propose to attribute a middle Miocene age to Subunit IC (Hole 1196A) based on the occurrence of *Miogypsina* spp.

F6. Uranium and resistivity log correlation, Holes 1196A and 1199A, p. 30.

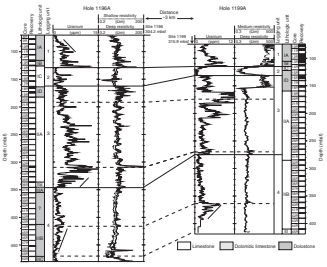

Site 1196

The studied vertical succession at Site 1196 comprises seven subunits (Fig. F5).

1. The upper part of Subunit IIIA (345.8–412.7 mbsf, Hole 1196A) consists of a pinkish white to light brown dolomitic limestone. The facies results from both recrystallization and dissolution of a poorly sorted rudstone-grainstone with massive and branching corals, mollusks, and rhodoliths. The lower part of Subunit IIIA is poorly recovered. It contains some intervals of white dolomitic floatstone with common to rare rhodoliths, red algae and echinoid fragments, bryozoans, and large hyaline benthic foraminifers in a grainstone matrix. The lower boundary of Subunit IIIA is defined by the appearance of a brilliant white sucrosic dolostone in the underlying Subunit IIIB.
2. Subunit IIB (335.9–345.8 mbsf, Hole 1196A) is a poorly sorted rudstone-boundstone with massive and thick lamellar coral colonies. Rare mollusks, red algae, and miliolids were observed in a medium to coarse sand-sized packstone-grainstone matrix. The lower boundary of Subunit IIB is lithologic in nature with dolomitization of the rocks.
3. Subunit IIA (182.2–335.9 mbsf, Hole 1196A) is a poorly sorted light gray to pale brown (yellow) floatstone in a silt-sized grainstone matrix. The subunit's predominant components are large porcellaneous benthic foraminifers (alveolinids and soritids), gastropods, and unbroken bivalves including pectinids, solitary corals, and bryozoans. Coral fragments of possible secondary reef frame builders (Table T1) occur especially in the lower part of the subunit. The grainstone matrix contains abraded red algae debris and small benthic foraminifers (miliolids). Threadlike dark patches up to 1 cm long were observed in the upper part of

the subunit. They were interpreted as preserved sea-grass roots (Shipboard Scientific Party 2002a, 2002b).

4. Subunit ID (162.8–182.2 mbsf, Hole 1196A; 145.0–184.9 mbsf, Hole 1196B) is a pale brown dolomitic floatstone in a grainstone matrix. Biogenic components are elongated fragments of branching red algae, rhodoliths, and large hyaline benthic foraminifers. Lamellar and branching coral fragments, bivalves, and bryozoans are also present. The lower boundary of Subunit ID corresponds to a sharp lithologic change with a thin dolomitic crust in Hole 1196B.
5. Subunit IC (125.9–162.8 mbsf, Hole 1196A; 130.5–145.0 mbsf, Hole 1196B) comprises light gray to white floatstone-rudstone and boundstone with hermatypic corals a few centimeters in size. Subordinate rudite-sized components are similar to those in Subunit ID. They are all included in a fine to medium grainstone matrix. The lower boundary of Subunit IC in Hole 1196A is described as an iron-stained, 1-cm-thick micritic crust (Shipboard Scientific Party, 2002b).
6. Subunit IB (117.2–125.9 mbsf, Hole 1196A; 122.9–130.5 mbsf, Hole 1196B) is a pale brown dolomitized floatstone-rudstone with predominantly elongated fragments of branching red algae in a recrystallized grainstone matrix. Subordinate rudite-sized components are molds of large hyaline benthic foraminifers, mollusks, and bryozoans. The lower boundary of Subunit IB consists of a sharp lithologic change.
7. Subunit IA (0–117.2 mbsf, Hole 1196A; 0–122.9 mbsf, Hole 1196B) is a white to pale brown (or yellow) dolomitic floatstone-rudstone with abundant rhodoliths as large as 10 cm in a grainstone matrix. Its subordinate rudite-sized components are lamellar coral colonies, molds of large hyaline benthic foraminifers, mollusks, and bryozoans. These bioclasts, together with red algae fragments, represent a moderately sorted and fine to medium sand matrix. Mud is only present as discontinuous laminae as thin as a few millimeters. A crude stratification with a fining upward trend is sometimes defined by small rhodolith layers. Corals become common upcore in the uppermost five cores, with either colonial secondary reef frame builders or solitary forms (Table T1). In Hole 1196A, the top of Subunit IA has an irregularly iron-stained surface. This surface is capped by a 1-cm-thick layer of wackestone with a planktonic foraminiferal assemblage of Pliocene age (Shipboard Scientific Party, 2002a).

Site 1199

The vertical succession at Site 1199 (Hole 1199A) is partly similar to those described at Site 1196. It comprises six subunits (Fig. F5).

Subunit IIB (285.0–410.0 mbsf) is a thick succession of white to pale yellow (dolomitic) limestone. It consists of meter-scale alternations of floatstones with rhodoliths as large as a few centimeters and well-sorted medium to coarse sand-sized grainstones. The biogenic components encountered include red algae fragments, hyaline larger benthic foraminifers, bivalves, gastropods, echinoid spines, and bryozoans. Coral fragments are present at the top of Subunit IIB in Core 194-1199A-39R. Its lower boundary corresponds to a gradual lithologic change to a 5-cm-thick white sucrosic dolostone. This facies was retrieved by the core catcher of the lowermost core (194-1199A-45R) from Hole 1199A. Sub-

unit IIB facies and the underlying sucrosic dolostone facies are very close to Subunits IIIA and IIIB facies from Hole 1196A, respectively.

Subunit IIA (159.8–285 mbsf) from Site 1199 is very similar to Subunit IIA from Site 1196. Its upper part consists of a pale brown, slightly dolomitized floatstone with large porcellaneous foraminifers, mollusks, solitary corals, and bryozoans in a silt-sized grainstone matrix. Its lower part also contains a noticeable amount of coral fragments of possible secondary reef frame builders (Table T1).

Subunit ID (121.9–159.8 mbsf) is a very pale brown to white dolomitic floatstone with a grainstone matrix. Biogenic components consist of a variable amount of elongated fragments of branching red algae, rhodoliths with associated bryozoans, and large hyaline benthic foraminifers as molds. Corals are locally present as branching colonies within rudstone layers. The top of Subunit ID corresponds to a 3-cm-thick red micritic layer rich in silt-sized quartz grains (Shipboard Scientific Party, 2002b).

Subunit IC (114.1–121.9 mbsf) is a very pale brown to light reddish dolomitized floatstone-rudstone and boundstone. The rocks are locally leached and infiltrated by reddish silt (Shipboard Scientific Party, 2002b). Biogenic components are fragments of branching red algae, molds of large hyaline benthic foraminifers, and massive and branching coral and rare rhodoliths as large as a few centimeters.

The last two subunits from Site 1199, IB (106.6–114.1 mbsf) and IA (0–106.6 mbsf), exhibit the same facies and thicknesses as Subunits IB and IA from Site 1196, respectively. Subunit IB is also a pale brown dolomitized floatstone with branching red algae in a recrystallized grainstone matrix. The only difference is the occurrence of rare corals. The lower boundary of Subunit IIB corresponds to a sharp lithologic change. Subunit IA is a white to pale brown (yellow) dolomitic floatstone-rudstone with centimeter-sized rhodoliths in a grainstone matrix. An increasing amount of coral upcore is also observed in the five uppermost cores. The coral assemblages are given in Table T1.

MICROFACIES ANALYSIS AND PALEOENVIRONMENTAL INTERPRETATION

The analysis of biogenic components and foraminiferal assemblages using the above methodology and the sedimentary features observed in cores and thin sections allowed six microfacies to be defined. These were labeled A through F, and their interrelationships were established (Fig. F7). The microfacies are given with their percentage in Figure F4 and are shown next to lithostratigraphic columns (Figs. F8, F9). The microfacies distribution at both Sites 1196 and 1199 does not follow a random pattern. Indeed, most of the microfacies are restricted to well-defined cored interval of lithostratigraphic subunits with respect to upcore variations of fossils assemblages (Fig. F5) and microscopic biogenic components (Figs. F8, F9). Microfacies uniformity suggests the stability of well-defined depositional settings and/or the prevalence of biosedimentological and environmental factors. As a consequence, an interpretation in terms of depositional setting is proposed with each microfacies description and is reported alongside the lithostratigraphic units (Fig. F5). Then, CFA is used to establish microfacies interrelationships in order to understand the upcore vertical microfacies succession with respect to environmental changes.

F7. CFA planes of axes 1-2 and 1-3 with microfacies and environmental interpretation, p. 31.

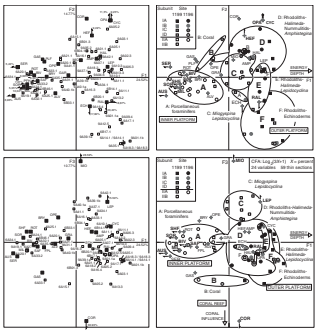

F8. Microfacies biogenic components vs. Site 1196 lithostratigraphic column, p. 32.

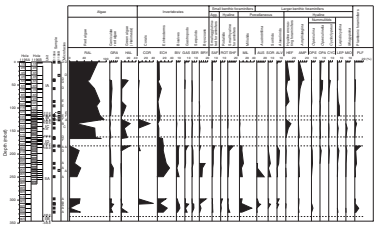

F9. Microfacies biogenic components vs. Site 1199 lithostratigraphic column, p. 33.

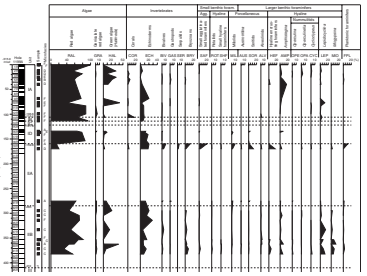

Microfacies Descriptions

Microfacies A: Porcellaneous Foraminiferal–Red Algal Packstone

This microfacies is present in Subunit IIA at both sites and in the upper part of Subunit ID or Subunit IC (Figs. F8, F9). This mud-poor packstone to floatstone is defined by porcellaneous foraminifers (1%–33%), small agglutinated foraminifers (1%–19%), small hyaline foraminifers (0%–13%), and bivalves (0%–9%). Red algae is sometimes the major component (0%–83%).

Microfacies A is especially characterized by large porcellaneous forms with *Austrotrillina howchini* (0%–18%), alveolinids (0%–5%) including *F. bontangensis,* and soritids (0%–23%) (Pl. P1, figs. 1, 2). These represent the coarse portion of sediment, together with scattered, unbroken gastropods and bivalves up to 1 cm in size, delicate branches of red algae, associated serpulid colonies, and the rare large hyaline foraminifers *Operculina*, *Lepidocyclina,* and *Miogypsina*. Plates of the green algae *Halimeda* are locally abundant (0%–38%), as are rounded endoclasts.

All these bioclasts are mixed in a moderately sorted silt to medium sand composed of numerous peletoids and micritized red algae, miliolids, echinoderms (6%–33%) (echinoid plates and spines and ophiurids ossicles), and mollusks. Subordinate small bioclasts are delicate-branched bryozoan colonies (0%–16%), small hyaline benthic foraminifers including rotaliids (0%–16%), epiplanktonic foraminifers (0%–14%) (orbulinids and globigeriniids), and geniculate red algae (0%–10%). Bioturbation occurs only within mud-rich packstones. Early marine cementation sometimes occurs around grains as thin isopachous rims of Mg calcite blades.

Paleoenvironmental Interpretation

The predominant fine-grained sediment in Microfacies A may be related to continuous winnowing by currents. Micritization and associated peloids suggest a long-time presence of grains. The variable mud and endoclast contents and unequal preservation of larger bioclasts attest to high- to moderate-energy settings. The geniculate red algae, soritids, alveolinids, and suspected sea-grass roots suggest sea-grass meadow areas. Using *Austrotrillina* and *Flosculinella*, Chapronière (1975) and Betzler and Chapronière (1993) assigned a shallow and protected platform environment to similar middle Miocene facies from Australia. Moreover, Chapronière (1975) proposed a water depth of <30 m for the foraminiferal assemblage. The facies and depositional settings were also found by Fournier et al. (2004) in an Oligocene–Miocene isolated platform in the Philippines. Microfacies A also shows similarities with the miliolid–small rotaliniid facies of modern restricted platform and lagoon settings defined by Hallock and Glenn (1986). However, the Microfacies A environment appears to be related to more open-ocean conditions, as numerous echinoderm fragments and epiplanktonic foraminifers are present. Thus, Microfacies A can be assigned to an inner but not restricted platform setting.

Microfacies B: Coral–Red Algal Rudstone-Floatstone

This microfacies is only represented by three thin sections sampled in Subunits IIA and at either the upper part of Subunit IC or the upper part of Subunit IA (Figs. F8, F9). This microfacies is defined by the oc-

P1. Floatstone-grainstone specimens, p. 38.

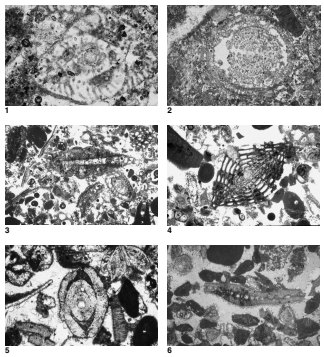

currence of scattered coral fragments of solitary and colonial taxa up to 1 cm in size (5%–40%) and abundant red algae (17%–59%). The corresponding coral assemblages are described in Table T1. The rudite-sized fraction of Microfacies B consists of thick-branched red algae, rhodoliths, micritized *Halimeda* plates (1%–24%), mollusks (2%–7%), and sporadic large benthic foraminifers (7%–13%). The silt to medium sand-sized portion of wackestone-packstone fabric shows dominant subangular to well-rounded red algae fragments, mixed with miscellaneous small benthic foraminifers (0%–7%), epiplanktonic foraminifers (1%–4%), and echinoid debris (1%–6%). A broad stratification with thin discontinuous laminae of micrite is visible in Unit I samples.

Paleoenvironmental Interpretation

Microfacies B likely represents a high- to moderate-energy environment within or near coral patch reefs, indicated by poorly sorted rudstone to wackestone textures and by the coral assemblages given in Table T1. These corals are second reef frame builders. In Subunits IIA and IC they are characteristic of low-energy and well-oxygenated environments. At the top of Subunit IA, they hold a high-energy significance.

Microfacies C: *Miogypsina-Lepidocyclina*–Red Algal Floatstone-Packstone

This microfacies is represented in Subunit IIB at Site 1199 (Fig. F9) and in one single sample at the base of a coral boundstone within Subunit IC at Site 1196 (Fig. F8). This microfacies exhibits upcore textural variations from floatstone-grainstone to packstone with common stratified geopetal deposits. It is characterized by *Miogypsina* (1%–12%) and, to a lesser extent, by *Lepidocyclina* (1%–13%) (Pl. P1, figs. 3, 4). It comprises an unsorted bioclastic sand with fragmented subangular to rounded branching red algae (32%–71%), geniculate red algae (0%–3%), branching bryozoan colonies (1%–8%), echinoderms (5%–20%) including ophiurids ossicles, and a noticeable amount of benthic foraminifers as large as 2 mm (6%–30%). Two foraminifer assemblages can be distinguished: one is an association of robust hyaline forms (common *Miogypsina*, *Lepidocyclina,* and *Amphistegina* and sporadically subordinate rotaliids and nummulitids such as *Cycloclypeus*, *Operculina,* and *Operculinella*), and the other one contains porcellaneous forms (alveolinids including *F. bontangensis*, soritids, and miliolids). *Halimeda* plates and bivalves (ostreids and pectinids) occur sporadically. Crusts made of branching red algae, lamellar bryozoan colonies, serpulid colonies, and encrusting hyaline foraminifers sometimes develop on a single side of large hyaline benthic forms (*Lepidocyclina)*. Other small benthic and epiplanktonic foraminifers are also present.

Paleoenvironmental Interpretation

The microfacies represents a high-energy setting indicated by the fragmentation and roundness of the individual bioclasts. The presence of large robust well-preserved hyaline benthic foraminifers suggests a high-energy, shallow-water environment (Hallock and Glenn, 1986). Microfacies C also contains a foraminifer assemblage of *Miogypsina*, *Lepidocyclina,* and *Cycloclypeus*. A similar microfacies from northwest Australia, dated early to middle Miocene, was reported by Chapronière (1975) to a shallow water depth of <50 m.

The common geniculate red algae and the porcellaneous foraminifer assemblage are similar to those of Microfacies A, which we assigned to sea-grass meadow influences. Sedimentation breaks, as exemplified by geopetal deposits and encrusted *Lepidocyclina*, and recurrent textural variations are indicative of periodic decreases of energy. These sedimentary features may be related to periodic storm action and/or debris flows. Martín and Braga (1993) and Martín et al. (1993) also report these two processes for a similar red algal facies of outer-platform settings, dated middle Miocene, from the Queensland and Marion plateaus. Finally, the lack of coral in Microfacies C suggests an outer-platform setting far away from reef influence.

Microfacies D: Nummulitids-*Amphistegina*-*Halimeda*-Rhodolithic Floatstone

The microfacies occurs in the upper parts of both Subunits IA and IIA at both Sites 1196 and 1199 and at the top of Subunit ID at Site 1196 (Figs. **F8, F9**). This unsorted floatstone to mud-poor packstone is defined by large, robust, and partly reworked hyaline benthic foraminifers including *Amphistegina* (1%–16%) and the nummulitids *Cycloclypeus* (0%–5%) and *Operculinella* (0%–2%) (Pl. **P1,** figs. 5, 6). Microfacies D is also characterized by red algae (20%–79%) and *Halimeda* plates (1%–31%). All these bioclasts compose a coarse amount of rhodoliths a few centimeters in size (except in Subunit IIA), encrusting hyaline foraminifers (0%–16%), and branching red algae. Solitary and colonial coral (0%–5%), mollusks (0%–7%), and well-preserved *Lepidocyclina* specimens 2 mm in size (0%–4%) occur sporadically. Sponge clionids mostly affect all these bioclasts, whereas rare bivalve borings are only observed in rhodoliths. The fine portion of the sediment contains echinoderms (1%–18%), subangular red algae fragments, and epiplanktonic foraminifers (0%–8%). Most of the bioclasts are fragmented, rounded, and slightly micritized. A broad stratification may occur with faint upward-fining layers a few centimeters thick. Each layer of wackestone-packstone fabric contains medium sand-sized particles followed by discontinuous wavy laminae of micrite <1 mm thick. Thin micritic-rimmed cement can develop on top of bioclasts and geopetal micritic infillings of pores. These cements are sometimes buried by another geopetal micritic deposit.

Paleoenvironmental Interpretation

Microfacies D indicates a high- to moderate-energy environment with occasional coral reef input. The presence of epiplanktonic foraminifers as well as the rich association of large hyaline benthic foraminifers and rarity of porcellaneous foraminifers suggests an outer-platform setting. The presence of several generations of geopetal deposit separated by micritic rims suggests sedimentation breaks. These sedimentary features with faint upward-fining layers may be characteristic of slope deposition controlled by sporadic storms. Indeed, Martín et al. (1993) reports a storm-influenced outer-platform setting at depths ranging from 30 to 80 m in an almost identical rhodolithic facies, dated middle Miocene from the Marion Plateau (Leg 133, Site 816). Marshall et al. (1998) also report depths ranging from 40 to 120 m for a comparable facies from a modern Australian environment. In the depositional environment inferred from the analysis of Microfacies D, the high percentage of *Halimeda* plates suggests the existence of meadows. Davies and Marshall (1985) and Drew and Abel (1988) reported finding *Hal-*

imeda meadows at depths ranging from 20 to 100 m in the Holocene to modern environments of the Great Barrier Reef Province.

Microfacies E: *Lepidocyclina-Halimeda*-Rhodolithic Floatstone

This unsorted floatstone to mud-poor packstone is present in the lower part of Subunit IA and in either Subunit IB or Subunit ID (Figs. F8, F9). It is characterized by especially large (up to 5 mm) and flat common *Lepidocyclina* (0%–11%), rare *Amphistegina* (0%–2%), and varying percentages of *Halimeda* plates (1%–41%). Red algae (40%–82%) is a major component with rudite-sized rhodoliths and delicate branches. The sand-sized portion of the sediment mainly contains red algae and echinoid fragments (0%–10%). The other bioclasts are rare and sporadic.

Paleoenvironmental Interpretation

Microfacies E exhibits the same fabric as microfacies D with prevalent red algae and *Halimeda* plates. The restricted large benthic foraminiferal assemblage, the lower amount of *Amphistegina*, and the absence, for the most part, of porcellaneous benthic foraminifers, encrusting hyaline foraminifers, and coral suggest an outer-platform setting in a deeper position with respect to Microfacies D. Such a deep setting may explain the occurrence of the especially large and flat, well-preserved specimens of *Lepidocyclina*. Indeed, the increasing size and degree of flatness of the benthic foraminifers can be related to light attenuation with increasing habitat depth (Hallock and Glenn, 1986). Nevertheless, the nature of substrate can also be a controlling factor (Hottinger, 1983). Finally, the presence of *Halimeda* plates with a similar percentage as Microfacies D and absent corals and porcellaneous foraminifers may reinforce the hypothesis of in situ *Halimeda* meadows in outer-platform settings.

Microfacies F: Echinoderm-Rhodolithic Floatstone

This unsorted floatstone to mud-poor packstone is mainly present in Subunits ID, IB, and IA (Figs. F8, F9). It contains abundant rhodoliths and branching red algae fragments (66%–99%) and a rudite-sized fraction of echinoderm debris with mainly echinoid plates and spines (1%–28%). The other rare and sporadic bioclasts are coral, nummulitids, alveolinids, small benthic and epiplanktonic foraminifers, and *Halimeda* plates.

Paleoenvironmental Interpretation

Microfacies F, as well as Microfacies D and E, may represent an outer-platform setting of high to moderate energy with respect to its fabric and red algae abundance. The paucity of small bioclasts, including benthic and planktonic foraminifers, is most likely due to winnowing. Low bioclast diversity and the absence of coral may indicate that the depositional setting is far away from reef influence.

Microfacies Interrelationships

Microfacies interrelationships are established according to significant biogenic components (variables) and environmental controlling factors using CFA. Results are illustrated in Figure F7.

Description

The first three axes calculated by the CFA explain 50.06% of the total variance of the data structure. These axes are controlled by 15 significant variables. The eigenvalues, relative inertia percentages of the axes, and the contributions of the variables are shown in Table T2. Examination of the factorial planes of axes 1 and 2 and axes 1 and 3 show a mostly continuous and homogeneous distribution of the samples (thin sections) (Fig. F7). Such a distribution indicates close interrelationships between microfacies with respect to significant variables, as shown in Figure F4.

Factorial axis 1 shows the opposition between a group of significant variables (*Austrotrillina*, soritids, miliolids, small hyaline foraminifers, small agglutinated foraminifers, bivalves, and serpulids) and a single variable (red algae) (Fig. F7). Within Microfacies A (porcellaneous foraminifers), the group of significant variables characterizes the biogenic composition of Subunit IIA and, to a lesser extent, Subunit IIB and that near the top of Subunits IC and ID (Figs. F8, F9). This first group of variables is also represented, but to a lesser extent, in Microfacies C and some thin sections of Microfacies B and D. On the contrary, red algae appears as a significant component of rhodolithic Microfacies D, E, and F, with the latter containing the highest percentage.

Factorial axis 2 classifies microfacies with respect to the opposition between the variables of red algae and echinoderms and the variables of *Operculinella* and *Cycloclypeus* (nummulitids) and encrusting hyaline foraminifers (Fig. F7). The upcore vertical succession along axis 2 of Microfacies F (red algae and echinoderms), E (*Halimeda* and *Lepidocyclina*), and D (*Halimeda*, nummulitids, and *Amphistegina*) is also visible at both Sites 1196 and 1199 in Subunits IA, IB, and ID (Figs. F8, F9).

Factorial axis 3 classifies microfacies with respect to coral and the variable pair *Miogypsina-Lepidocyclina*, which allows the discrimination of Microfacies B and C, respectively. Microfacies C is mostly represented within Subunit IIB at Site 1199 (Fig. F9).

Interpretation

A bell-shaped distribution of samples tends to appear on the factorial planes of axes 1 and 2 and of axes 1 and 3 (Fig. F7). Such a distribution may represent a possible polynomial relationship between axes, called the "arch" effect or "Guttmann" effect, and it is classically considered to be the manifestation of environmental gradients along a factorial axis (Hennebert and Lees, 1991). The Guttmann effect is visualized along axis 1 by the succession of Microfacies A–F.

Based on the microfacies descriptions and environmental interpretations, the bell-shaped distribution may correspond first to a depth gradient along axis 1. Axis 2 appears to be linked to axis 1 and does not hold any environmental significance. Indeed, Microfacies A (porcellaneous foraminifers) of the inner-platform setting is opposed to the three rhodolithic Microfacies D, E, and F of the outer-platform setting along axis 1. Microfacies C most likely holds an intermediate depth significance as it contains porcellaneous foraminifers, as does Microfacies A, and thus may register inner-platform influences. A gradual transition between depositional settings of Microfacies A and C may exist as both microfacies occur at Site 1199 in lithostratigraphic Unit II and are interlayered. This is also the case for Microfacies D–F as they are interlayered in Subunits IA and IB.

Moreover, axis 1 may correspond to both an energy gradient and a winnowing gradient. Indeed, the prevalent granulometry increases along the arch of the factorial plane of axes 1 and 2. Thus, the granulometry consists of silt to fine sand in Microfacies A, medium to coarse sand in Microfacies C, and coarse sand with additional numerous rhodoliths a few centimeters in size in Microfacies D through F. On the contrary, the fine portion of sediment including mud tends to disappear along the arch. The gradual disappearance of small bioclasts, including small benthic and planktonic foraminifers, from microfacies D to F can be also related to an increasing winnowing process.

Finally, axis 3 may represent a coral influence gradient (Fig. F7). Indeed, coral occurs in Microfacies B and in some thin sections of Microfacies D, whereas it is absent in Microfacies C.

The CFA ordering of Microfacies A–F along the arch is also associated with a reduction in the diversity of biogenic components, as shown in Figure F4. This phenomenon can be related to gradients of winnowing, depth, and coral influence. Indeed, an upcore vertical succession from Microfacies F and E to Microfacies D occurs in Subunits IA and IB at both Sites 1196 and 1199. This is consistent with the occurrence of common coral pebbles in the five uppermost cores at both sites in Subunit IA, whereas coral is absent in Subunit IB (Fig. F5).

Thus, the CFA ordering of Microfacies A–F with respect to the environmental gradients is representative of the upcore vertical biosedimentary evolution at both Sites 1196 and 1199 (Fig. F5). As a consequence, the microfacies evolution will be examined along with the site lithostratigraphic units with respect to the CFA ordering.

DISCUSSION

Depositional Architecture

The combination of the microfacies results and the lithologic synthesis with the available seismic and stratigraphic data set from the Shipboard Scientific Party (2002a, 2002b) allowed us to refine the depositional architecture of the SMP on a regional scale (>5 km). In addition, we will define the geometry of some sedimentary bodies on a smaller scale (a few hundred meters).

SMP's Depositional Architecture

Based on seismic analysis, stratigraphy, and biosedimentology, the Shipboard Scientific Party (2002a) established the depositional architecture at the scale of the SMP (>5 km). They described an asymmetrical platform with a northwestern flat-topped, reef-rimmed margin and an evolving southeastern margin from a distally steepened to a more homoclinal ramp (Fig. F3). In this pattern, they related the asymmetrical platform architecture to the strong influence of currents from the north to the south. In addition, the Shipboard Scientific Party (2002a) inferred a water depth increase and a coral reef–development decrease toward the southwest. Thus, Sites 1196 and 1199 were drilled in the flat-topped inner part of the platform behind a possible reef rim. Such a depositional architecture with rimmed platform and ramps has already been described or inferred from seismic analysis and biosedimentological studies in other Cenozoic carbonate platforms from Australia and the Indian Pacific Ocean (e.g., Chapronière, 1975; Betzler, 1997; Mar-

shall et al., 1998; Noad, 2001; Fournier et al., 2004). Nevertheless, our analysis of the SMP's coral assemblages cannot reinforce the hypothesis of a well-developed reef rim because no primary framebuilders were found at Sites 1196 and 1199, as shown in Table **T1.**

The Shipboard Scientific Party (2002a, 2002b) considered the SMP's lithostratigraphic succession to be mostly monoclinal from one site to the other. They also demonstrated that the corresponding subunits showed very similar sedimentary facies, fossil assemblages, and thicknesses (Figs. **F3, F5**).

Our statistical analysis of microfacies partly confirms the lithostratigraphic subdivisions. Indeed, the composition and evolution of microfacies are mostly identical in each of the subunits represented within both sites (Fig. **F5**). Nevertheless, some exceptions remain for Subunits IC, ID, and IIB. Indeed, the microfacies composition and the fossil assemblages of these subunits signal the influence of coral reefs and rather support the alternative logging stratigraphy (Figs. **F5, F6**). In the logging stratigraphy, the boundary between logging Units 3 and 2 represents a gradual sedimentary change from rhodolithic floatstones (Microfacies D, E, and F) to coral boundstones-floatstones (Microfacies B and A) within Hole 1199A (Fig. **F5**). The boundary between the logging Units 3 and 4 and the dashed boundary situated just upcore in logging Unit 3 (Fig. **F6**) represent a gradual sedimentary change from large hyaline benthic foraminiferal floatstones (Microfacies C), coral boundstones-rudstones (Microfacies B), and porcellaneous foraminiferal grainstones (Microfacies A). Further, Subunit IIB and the coral upper part of Subunit IIIA (Hole 1196A) are correlated to the coral lower part of Subunit IIA (Hole 1199A), with respect to the logging stratigraphic pattern (Fig. **F5**). Finally, the lower part of Subunit IIIA (Hole 1196A) is correlated to Subunit IIB (Hole 1199A) (Fig. **F5**). At both sites, a dolomitic sucrosic facies appears at ~410 mbsf (Fig. **F5**). This facies most likely corresponds to the top of the old dolomitic platform, mostly dated early Miocene in age by the Shipboard Scientific Party (2002a) (Fig. **F3**). Further, the studied 410-m-thick stratigraphic succession may be subdivided into two parts with respect to the composition of microfacies and sedimentary rocks. The lower part would include Unit II and Subunit IIIA, and the upper part would correspond to Unit I.

Geometry of Sedimentary Bodies

A seismic profile a few hundred meters long provides well-defined seismic reflections in the 200-m-thick uppermost part of the platform succession at Site 1196 (Fig. **F10**). The analysis of these reflections suggests the existence of lens-shaped sedimentary bodies as thick as 30 m and prograding clinoforms in lithostratigraphic Unit I (Fig. **F10**). Such a sedimentary architecture supports the Shipboard Scientific Party's (2002b) observation of lateral variations as much as 20 m thick in Subunits IC and ID from Holes 1196A to 1199A, which lie at a distance of 20 m. Indeed, the difference of the thickness between the two holes was considered significant, as it exceeds the depth errors due to coring (Shipboard Scientific Party, 2002b).

Several sedimentary features encountered at both Sites 1196 and 1199 are also consistent with the seismic architecture. Thus, some cross-bedded stratifications underlined by rhodolithic layers were observed in core sections from Unit I (Shipboard Scientific Party, 2002b). These stratifications may correspond to the clinoforms suspected in the seismic profile (Fig. **F10**). The occasional grading of sediments with recur-

F10. Seismic reflections of Line MAR07, Site 1196, p. 34.

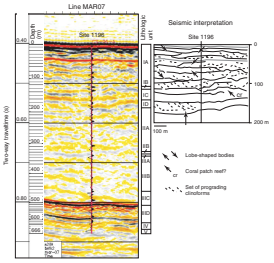

rent textural variations, the sedimentation breaks as exemplified by several generations of geopetal deposits, and the winnowing of the fine sand portion of sediment found in the rhodolithic Microfacies D, E, and F of Unit I can be characteristic of debris flows in slope settings. These sedimentary features may characterize the progradation of the clinoforms that are a response to strong currents that are inferred from the SMP's asymmetrical architecture by the Shipboard Scientific Party (2002a). These sedimentary features may also be associated with reef talus deposition. Indeed, an upcore gradual change in sedimentation occurs from rhodolithic floatstones to coral rudstones-boundstones in Subunits ID and IC at both sites. The presence of coral boundstones in Subunit IC at both sites points to the settlement of coral reefs at the SMP's scale. The available seismic data provide poor information of the geometry of these coral reefs. Nevertheless, some reflections may be interpreted as 200-m-long and 20-m-thick lens-shaped bodies (Fig. **F10**).

Although the association of both coral and rhodolithic facies have been documented in Cenozoic and modern platforms from Australia (e.g., Betzler, 1997; Davies, McKenzie, Palmer-Julson, et al., 1991; Davies and Peerdeman, 1998; Marshall et al., 1998), the geometry of the sedimentary bodies is poorly illustrated at a small scale. On the contrary, the geometry of a set of clinoforms, possibly similar to those of the SMP, is well known in some rhodolithic distally steepened ramps, dated late Miocene, from the Mediterranean region. Thus, Pomar et al. (1996) and Pomar (2001) reported a set of 2-km-long and 40-m-thick clinoforms in a 20-km-long prograding rhodalgal ramp from the Balearic Islands (Spain). In addition, Saint Martin et al. (1997) characterized a vertical stacking set of clinoforms 1–4 km long and 10–30 m thick in a 10-km-long prograding rhodalgal ramp from the Maltese Islands. Within this ramp, the clinoforms exhibit scattered lens-shaped coral reefs at the toes of their topsets.

Finally, the definition of the seismic profile did not really allow us to discern the sedimentary architecture of lithostratigraphic Unit II (Fig. **F10**). Nevertheless, the large hyaline foraminiferal deposits (Microfacies C) of Subunit IIB (Site 1199) and Subunit IIIA (Site 1196) indicate the existence of slope deposition as do the three rhodolithic microfacies (D, E, and F) from Unit I. On the contrary, no sedimentary features characteristic of slope deposition were observed in the porcellaneous foraminiferal deposits (Microfacies A) of Subunit IIA. Chapronière (1975) reported similar porcellaneous foraminiferal deposits in subhorizontal beds, dated middle Miocene, from western Australia.

Reconstruction of Depositional Environments

The reconstruction of depositional environments is necessary to better understand the biosedimentary and paleoenvironmental evolution of the SMP at Sites 1196 and 1199. Based on the microfacies analysis, the corresponding paleoenvironmental interpretations, and the stratigraphic data, we defined an upcore vertical succession of six depositional environments at both sites (Fig. **F5**). Further, we proposed two reconstructions for Unit II–Subunit IIIA and Unit I, respectively (Fig. **F11**). The reconstructions correspond to the two main lithostratigraphic subdivisions of the vertical succession at both sites. They represent a theoretical zonation of platform deposits on the scale of the sedimentary bodies (at most 1 km in length) with repartitioned microfacies and the corresponding depositional environments. These reconstructions take into account the seismic architecture, the biosedi-

F11. SMP depositional environment reconstruction, p. 35.

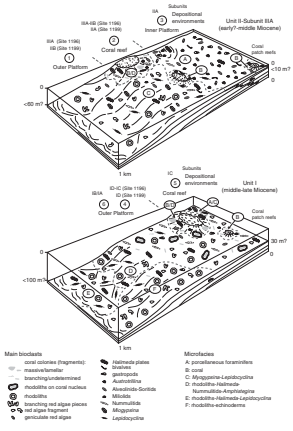

mentological data synthesized in the site lithostratigraphic columns (Fig. F5), and the results of the microfacies analysis. Thus, the repartitioned microfacies in each reconstruction is inferred from the microfacies' interrelationships with respect to the environmental gradients defined by the CFA (Fig. F7) and from their vertical succession and interlayering next to the site lithostratigraphic columns (Fig. F5). The close interrelationships of the microfacies and the gradual sedimentary evolution of the corresponding deposits at Sites 1196 and 1199 suggest a lateral coexistence of the superimposed depositional environments. Finally, one must note that these reconstructions illustrate only a restricted area of the inner part of the SMP, limited at its northeastern side by a possible reef rim (Shipboard Scientific Party, 2002a).

Depositional Environments of Unit II–Subunit IIIA

The proposed reconstruction illustrates a theoretical platform setting with the depositional environments of outer platform, coral reef, and inner platform (Fig. F11). The corresponding deposits and microfacies are superimposed and show gradual changes along the vertical succession of Subunits IIIA–IIB and IIA at Sites 1196 and 1199 (Fig. F5). Nevertheless, the geometry of the sedimentary deposits remains in question, as no well-defined seismic data are available. Consequently, our reconstruction also takes into account some other Cenozoic environmental models from Australia and the Indo-Pacific region, which exhibit comparable facies and biogenic components (Chapronière, 1975; Hallock and Glenn, 1986; Betzler and Chapronière, 1993; Fournier et al., 2004).

With respect to our microfacies results, the inner platform corresponds to a moderate- to high-energy environment under open-ocean influences. The prevalent porcellaneous foraminiferal fine sand (Microfacies A) deposits are only represented in Subunit IIA. Chapronière (1975) assigned a maximum water depth of 30 m to a comparable foraminiferal assemblage from Australia. The deposits are winnowed, probably from the action of bottom currents. Muddier fine sands are present and may be related to a sheltering effect of sea-grass meadows and scattered coral patch reefs (Microfacies B). The coral reef environment is also of high to moderate energy with respect to the coral assemblages. The deposits are a mixture of porcellaneous foraminiferal fine sands and coral–red algal coarse sands (Microfacies B and D) that are encountered in Subunits IIIA–IIB (Site 1196) and Subunit IIA (Site 1199). The outer-platform environment shows episodic variations of energy and sedimentary breaks, which we attributed to slope deposition and/or storm action. The prevalent deposits are unsorted *Miogypsina-Lepidocyclina* sands (Microfacies C) represented in Subunits IIB (Site 1199) and IIIA (Site 1196). We assigned a maximum water depth of 50–60 m to this large, hyaline foraminiferal assemblage, following the models of Chapronière (1975) and Hallock and Glenn (1986). Finally, these deposits register the influence of coral reef and inner-platform environments as they contain rare coral and a porcellaneous foraminiferal assemblage similar to those of Microfacies A.

Thus, we relate the existence of the inner-platform environment to the development of coral reefs as shown by others studies for similar depositional settings (e.g., Hallock and Glenn, 1986; Betzler and Chapronière, 1993; Robertson, 1998; Fournier et al., 2004). In these studies, the coral reefs form a reef rim and sometimes surround an inner-platform area (Robertson, 1998; Fournier et al., 2004). Although a reef rim is reported at the northwestern side of the SMP (Shipboard Scientific

Party, 2002a), the extension and the nature of the coral reef environment cannot be more precisely defined at Sites 1196 and 1199.

Depositional Environments of Unit I

The proposed reconstruction illustrates a theoretical platform setting with the depositional environments of outer platform and coral reef (Fig. F11). The corresponding deposits and microfacies are represented in three subunits (IA, IB, and ID) and in single Subunit IC (Fig. F5). The reconstruction of the sedimentary architecture takes into account the available seismic data (Fig. F10). Thus, the deposits characterized by the three rhodolithic microfacies (D, E, and F) correspond to several sets of prograding clinoforms. The coral boundstones (Microfacies B) coincide partly with lens-shaped bodies we interpreted as possible coral reefs (Fig. F10). Nevertheless, the exact geometry of the sedimentary bodies still remains hypothetical and needs more detailed seismic data to be precisely established. Thus, our reconstruction also takes into account some other Cenozoic environmental models from the Mediterranean region, which show similar geometry, facies, and biogenic components (Pomar et al., 1996; Saint Martin et al., 1997; Robertson, 1998; Pomar, 2001).

With respect to our microfacies results, the outer platform consists of a high- to moderate-energy environment with common sedimentary breaks, which we attribute to slope deposition controlled by sporadic storms. The prevalent deposits are coarse sands with numerous rhodoliths as large as 10 cm (Microfacies F). These deposits sometimes include either additional derived reefal material with coral fragments and reworked *Amphistegina*-Nummulitids (Microfacies D) or additional large and flat *Lepidocyclina* (Microfacies E), possibly indicative of great depths (Fig. F11). In addition, high numbers of *Halimeda* plates are present within Microfacies D and E, possibly indicating the existence of *Halimeda* meadows, as is the case at depths ranging from 20 to 100 m in Holocene to modern environments from the Great Barrier Reef (Davies and Marshall, 1985; Drew and Abel, 1988). Martín et al. (1993) assigned a storm-influenced outer-platform setting at depths ranging from 30 to 80 m to such rhodolithic facies from the Northern Marion Plateau. The coral reef environment might be represented by the development of coral patch reefs in a moderate- to high-energy setting. The prevalent deposits are coral boundstones-rudstones (Microfacies B) and rhodolithic coarse sands (Microfacies D); both are encountered in Subunit IC. The other rare deposits are benthic foraminiferal sands (Microfacies A and C), which may be indicative of a sheltered reefal environment. The coral environment might represent a lateral extension of the reef rim of the northwestern side of the SMP.

Evolution of Facies and Environments

Defining and ordering the six microfacies (A–F) with respect to their depositional signature from the inner platform, coral reef, and outer platform allowed the construction of a microfacies and environmental curve next to the lithostratigraphic columns of Sites 1196 and 1199 (Fig. F5). We recognized an almost identical succession of six depositional environments at both sites:

1. An outer-platform environment that is characterized by red algal-*Miogypsina-Lepidocyclina* sands and the absence of coral (Site

1196: Subunit IIIA; Site 1199: Subunit IIB, Microfacies C). We interpreted a maximum water depth of 50–60 m, based on the foraminiferal assemblage.
2. A coral reef environment that may be represented by coral patch reefs (Site 1196: Subunits IIIA–IIB; Site 1199: Subunit IIA, Microfacies B).
3. An inner-platform environment that is under the influence of possible scattered coral patch reefs (Sites 1196 and 1199: Subunit IIA). Its transition from the previous coral reef environment is gradual. The prevalent deposits are porcellaneous foraminiferal fine sands (Microfacies A) with occasional coral (Microfacies B), which are interpreted to occur at a maximum water depth of 30 m.
4. An outer-platform environment (Site 1196: Subunits ID–IC; Site 1199: Subunit ID), which strongly contrasts with the previous inner-platform environment. The prevalent deposits are rhodolithic coarse sands (Microfacies F and E). They also contain an amount of coral that increases upcore (Microfacies D). The rhodolithic facies is assigned to water depths ranging from 30 to 80 m.
5. A coral reef environment that has possible scattered coral patch reefs (Sites 1196 and 1199: Subunit IC). The transition from the previous outer-platform environment is gradual and may be already recorded in the deposits of Subunit ID. The prevalent deposits are interbedded coral boundstones-rudstones (Microfacies A and B) and rhodolithic coarse sands with coral (Microfacies D).
6. An outer-platform environment (Sites 1196 and 1199: Subunits IB–IA) that has a prevalent rhodolith facies was assigned to water depths ranging from 30 to 80 m. The deposits are devoid of coral (Microfacies F and E) in Subunit IB and in the lower part of Subunit IIA. They strongly contrast with the underlying coral deposits of Subunit IC. The upper part of Subunit IIA records an increasing coral reef influence (Microfacies D), indicative of an upward-shallowing general trend.

Thus, most of the changes of facies and environments clearly coincide with either the lithostratigraphic or logging stratigraphic subdivisions of the SMP proposed by the Shipboard Scientific Party (2002a, 2002b) (Fig. F5). The Shipboard Scientific Party (2002a, 2002b) described most of the retrieved boundaries as iron-stained micritic crusts a few centimeters thick. They interpreted the crusts as the result of hardground development following a possible exposure. Nevertheless, no unquestionable diagenetic features were found in thin sections to remove uncertainties about the existence of exposure (Shipboard Scientific Party, 2002b) Therefore, it has been stressed that additional diagenetic and isotopic studies will be necessary to refine the origin of the boundaries (Shipboard Scientific Party, 2002b).

Sea Level Variations

The analysis of the facies and environmental evolution, with respect to the stratigraphic subdivisions at both sites, points to the existence of three main shallowing sequences that are intercalated with three abrupt deepening events (Fig. F5).

Sequence 1 corresponds to Subunits IIIA, IIB, and IIA and is represented by a gradual evolution of environments from (1) outer platform,

(2) coral reef, and (3) inner platform. Using biostratigraphy from Boudagher-Fadel and Banner (1999), the upper part of the sequence (Subunit IIA) can be dated middle Miocene based on the foraminiferal assemblage of *Austrotrillina howchini* and *F. bontangensis*. On the contrary, the early middle Miocene age attributed to Subunits IIIA–IIB by the Shipboard Scientific Party (2002a, 2002b) cannot be determined with precision.

Sequence 2 corresponds to Subunits ID and IC, recording the succession from (4) an outer-platform environment to (5) a coral reef environment. The onset of this sequence is marked by an abrupt deepening with respect to the underlying inner-platform environment of Subunit IIA. The Shipboard Scientific Party (2002a, 2002b) reported iron-stained micritic crusts a few centimeters in thickness at the tops of both Subunits ID and IC. They attributed the boundary between Subunits ID and IC to the major late middle Miocene (N12–N14) sea level fall (Haq et al., 1988). This sea level fall was estimated in the Northern Marion Plateau at 86 m ± 30 mbsl (Shipboard Scientific Party, 2002a). However, we question the occurrence of such an event at this lithostratigraphic level. Indeed, our facies analysis instead showed a gradual biosedimentary evolution from Subunit ID to Subunit IC, which is more consistent with the alternative logging subdivisions of the Shipboard Scientific Party (2002b) (Figs. **F5, F6**). Moreover, the overlying Subunit IC contains unreworked larger benthic foraminifers *Miogypsina* spp. The last occurrence of this genus is positioned at the upper end of the planktonic Zone N12 or in the lower part of Zone N13 for the Indo-Pacific (Boudagher-Fadel and Banner, 1999; Boudagher-Fadel et al., 2000a). Thus, we propose instead to relate the surface between Subunits IC and IB to this second-order event. This surface would thus correspond to the Megasequence B/C seismic boundary, dated through seismic correlations to ~11 Ma by the Shipboard Scientific Party (2002a).

Sequence 3 occurs in Subunits IB and IA and is characterized by (6) an outer-platform environment. The onset of this sequence is marked by an abrupt deepening with respect to the underlying coral reef environment of Subunit IC. The lower part of the sequence is devoid of coral inputs, whereas its upper part shows the increasing influence of a coral reef environment. The Shipboard Scientific Party (2002a, 2002b) described at the top of Subunit IA an iron-stained irregular surface, overlain by laminated ferromanganese crusts and/or planktonic wackestone deposits, which they dated Pliocene in age. Further, they assumed that this surface coincides with the Megasequence C/D seismic boundary they dated to ~7.2 Ma and the drowning of the SMP. Thus, Sequence 3 occurred during the early late Miocene.

The correlation of the three shallowing sequences and the three deepening events to a global sea level curve remains problematic regarding potential high sea level variations during the middle and late Miocene (Haq et al., 1988). Sequences 1 and 2 of middle Miocene age record two shallowing phases that are intercalated with an abrupt deepening event. The sequences may correspond to two third-order cycles associated with the global middle Miocene sea level fall. The end of this event is represented at the SMP by an unconformity at the top of Sequence 2. Sequence 3, dated early late Miocene in age, represents a general shallowing consecutive to an abrupt deepening event with respect to the underlying coral reefs of Sequence 2. Thus, Sequence 3 may correlate to one of the third-order cycles following the major second-order sea level fall. Finally, the top of Sequence 3 was partly related to the

Pliocene drowning of the Marion Plateau (Pigram et al., 1992; Pigram, 1993; Shipboard Scientific Party, 2002a).

In the adjacent Queensland Plateau, depositional sequences of carbonate platform were established and the sea level variations were estimated from the middle Miocene to the Pliocene (Davies, McKenzie, Palmer-Julson, et al., 1991; Brachert et al., 1993; Betzler et al., 1993, 1995; Betzler, 1997). Nevertheless, a precise correlation of the platform deposits from the Queensland and Marion plateaus remains difficult to establish with respect to the biostratigraphic resolution and core recovery. Only some global events can be recognized in both areas. Thus, two deepening events occurring in the early late Miocene and in the Pliocene are reported in the Queensland Plateau (Betzler et al., 1995; Betzler, 1997). They may correlate to the two deepening events present at the tops of Sequences 2 and 3 from the Southern Marion Plateau. Finally, the effect of the second-order sea level fall (late middle Miocene in age) was also detected in the Queensland Plateau, particularly from the basinward shift in onlap along seismic profiles (Davis, McKenzie, Palmer-Julson, et al., 1991).

CONCLUSION

Petrographic facies analysis and supporting statistical analysis of the SMP (Sites 1196 and 1199) revealed the following:

1. The correlation pattern of Sites 1196 and 1199 was refined. The proposed lithostratigraphic subdivisions best match the logging subdivisions of the Shipboard Scientific Party (2002b).
2. The age of Subunits IC and ID was determined. A middle Miocene age is proposed, based on the occurrence of the genera *Miogypsina* in Subunit IC.
3. Two reconstructions of the depositional environments at a fine scale (1 km) were proposed in order to visualize the biosedimentary and environmental evolution of the inner part of the SMP. The inferred depositional environments range from inner platform and coral reef to outer platform.
4. SMP sedimentation registered three shallowing sequences followed by three deepening events during the middle Miocene to Pliocene time interval. The major late middle Miocene sea level fall (N12–N14) may correspond to the Subunit IC/IB boundary rather than to that of the Subunit ID/IC boundary.

ACKNOWLEDGMENTS

This research used samples and data provided by the Ocean Drilling Program (ODP). ODP is sponsored by the U.S. National Science Foundation (NSF) and participating countries under management of Joint Oceanographic Institutions (JOI), Inc. Funding for this research was provided by ODP France and by the French Institut National des Sciences de l'Univers–Centre National de la Recherche Scientifique (INSU-CNRS) "ad hoc OCEANS" Program 2001–2003. We are grateful to C. Papy and L. Marié for thin section preparation. We are grateful to F. Samrad for critically reading the manuscript. We thank J.P. André, G. Cabioch, C. Betzler, and J. Reijmer for their helpful reviews of the manuscript.

REFERENCES

Adams, C.G., 1968. A revision of the foraminifer genus *Austrotrillina* Parr. *Bull. Br. Mus. (Nat. Hist.), Geol.,* 16:71–97.

Beauvais, L., Chaix, C., Lathuilière, B., and Lauser, L., 1993. Morphological terms for describing Scleractinian: preliminary list [English translation by B. Rosen]. *Fossil Cnidaria,* 22:50–72.

Benzécri, J.P., 1980. *L'analyse des Données, II. L'analyse des Correspondances* (3rd ed.): Paris (Dunod).

Betzler, C., 1997. Ecological control on geometries of carbonate platforms: Miocene/Pliocene shallow-water microfaunas and carbonate biofacies from the Queensland Plateau (NE Australia). *Facies,* 37:147–166.

Betzler, C., Brachert, T.C., and Kroon, D., 1995. Role of climate in partial drowning of the Queensland Plateau carbonate platform (northeastern Australia). *Mar. Geol.,* 123:11–32.

Betzler, C., and Chapronière, G.C.H., 1993. Paleogene and Neogene larger foraminifers from the Queensland Plateau: biostratigraphy and environmental significance. *In* McKenzie, J.A., Davies, P.J., Palmer-Julson, A., et al., *Proc. ODP, Sci. Results,* 133: College Station, TX (Ocean Drilling Program), 51–66.

Betzler, C., Kroon, D., Gartner, S., and Wei, W., 1993. Eocene to Miocene chronostratigraphy of the Queensland Plateau: control of climate and sea level on platform evolution. *In* McKenzie, J.A., Davies, P.J., Palmer-Julson, A., et al., *Proc. ODP, Sci. Results,* 133: College Station, TX (Ocean Drilling Program), 281–289.

Boichart, R., Burollet, P.S., Lambert, B., and Villain, J.M., 1985. La plate-forme carbonatée de Pater Noster (Est de Kalimantan, Indonésie): étude sédimentologique et écologique. *Notes et Mémoires de Total CFP,* Paris, 20:1–103.

Boudagher-Fadel, M.K., and Banner, F.T., 1999. Révision de la signification stratigraphique des étages-lettres de l'Oligocène–Miocène. *Rev. Micropaléont.,* 42:93–97.

Boudagher-Fadel, M.K., Lord, A.R., and Banner, F.T., 2000a. Some Miogypsinidae (foraminifera) in the Miocene of Borneo and nearby countries. *Revue Paléobiol.,* 19:137–156.

Boudagher-Fadel, M.K., Noad, J.J., and Lord, A.R., 2000b. Larger foraminifera from late Oligocene–earliest Miocene reefal limestones of northeast Borneo. *Rev. Esp. Micropaleontol.,* 32:341–361.

Brachert, T.C., Betzler, C., Davies, P.J., and Feary, D.A., 1993. Climatic change: control of carbonate platform development (Eocene–Miocene, Leg 133, northeastern Australia). *In* McKenzie, J.A., Davies, P.J., Palmer-Julson, A., et al., *Proc. ODP, Sci. Results,* 133: College Station, TX (Ocean Drilling Program), 291–300.

Cahuzac, B., and Chaix, C., 1996. Structural and faunal evolution of Chattian–Miocene reefs and corals in western France and northeastern Atlantic Ocean. *In* Franseen, E., Esteban, M., Ward, W., and Rouchy, J.M. (Eds.), *Models for Carbonate Stratigraphy from Miocene Reef Complexes of the Mediterranean Regions*. Spec. Publ.—SEPM, 5:105–127.

Chaix, C., Moissette, P., and Saint Martin, J.P., 1986. Réflexions sur les biocénoses et paléobiocénoses en milieu récifal (Messinien d'Algérie). *Bull. Mus. Natl. Hist. Nat., Sect. C,* 8(2):219–230.

Chapronière, G.C.H., 1975. Palaeoecology of Oligo–Miocene larger foraminiferida, Australia. *Alcheringa,* 1:37–58.

Chapronière, G.C.H., and Betzler, C., 1993. Larger foramineral biostratigraphy of Sites 815, 816, and 826, Leg 133, northeastern Australia. *In* McKenzie, J.A., Davies, P.J., Palmer-Julson, A., et al., *Proc. ODP, Sci. Results,* 133: College Station, TX (Ocean Drilling Program), 39–49.

Coleman, P.J., 1963. Tertiary larger foraminifera of the British Solomon Islands, southwest Pacific. *Micropaleontology,* 9:1–38.

Cugny, P., and Rey, J., 1981. Analyse factorielle et nuées dynamiques appliquées à l'étude de biofaciès et de leurs enchaînements séquentiels: exemple de l'Albien portugais. *Geobios,* 14:311–321.

Davies, P.J., and Marshall, J., 1985. *Halimeda* bioherms—low energy reefs, northern Great Barrier Reef. *Proc. 5th Coral Reef Symp.,* 5:1–7.

Davies, P.J., McKenzie, J.A., Palmer-Julson, A., et al., 1991. *Proc. ODP, Init. Repts.,* 133 (Pts. 1, 2): College Station, TX (Ocean Drilling Program).

Davies, P.J., and Peerdeman, F.M., 1998. The origin of the Great Barrier Reef—the impact of Leg 133 drilling. *Spec. Publ. Int. Assoc. Sedimentol.,* 25:23–38.

Davies, P.J., Philip, A.S., Feary, D.A., and Pigram, C.J., 1989. The evolution of the carbonate platforms of northeast Australia. *In* Crevello, P.D., Wilson, J.L., Sarg, J.F., and Read, J.F. (Eds.), *Controls on Carbonate and Basin Development.* Spec. Publ.—SEPM (Soc. Sediment. Geol.), 44:233–258.

Ditlev, H., 1980. *A Field Guide to the Reef-Building Corals of the Indo-Pacific:* Rotterdam (W. Backhuys), 1–291.

Drew, E.A., and Abel, K.M., 1988. Studies on *Halimeda,* I. The distribution and species composition of *Halimeda* meadows throughout the Great Barrier Reef province. *Coral Reefs,* 6:195–206.

Etter, W., 1999. Community analysis. *In* Harper, D.A.T. (Ed.), *Numerical Palaeobiology:* Chichester (J. Wiley and Sons), 285–360.

Fournier, F., Montaggioni, L., and Borgomano, J., 2004. Paleoenvironments and high-frequency cyclicity from Cenozoic southeast Asian shallow-water carbonates: a case study from the Oligo–Miocene buildups of Malampaya (offshore Palawan, Philippines). *Mar. Petrol. Geol.,* 21:1–21.

Hallock, P., and Glenn, E.C., 1986. Larger foraminifera: a tool for paleoenvironmental analysis of Cenozoic carbonate depositional facies. *Palaios,* 1:55–65.

Haq, B.U., Hardenbol, J., and Vail, P.R., 1988. Mesozoic and Cenozoic chronostratigraphy and cycles of sea-level change. *In* Wilgus, C.K., Hastings, B.S., Kendall, C.G. St.C., Posamentier, H.W., Ross, C.A., and Van Wagoner, J.C. (Eds.), *Sea-Level Changes—An Integrated Approach.* Spec. Publ.—SEPM (Soc. Sediment. Geol.), 42:72–108.

Hennebert, M., and Lees, A., 1991. Environmental gradients in carbonate sediments and rocks detected by correspondence analysis: examples from the Recent of Norway and the Dinantian of southwest England. *Sedimentology,* 38:623–642.

Hottinger, L., 1983. Processes determining the distribution of larger Foraminifera in space and time. *Utrecht Micropaleontol. Bull.,* 30:239–253.

Isern, A.R., McKenzie, J.A., and Müller, D.W., 1993. Paleoceanographic changes and reef growth off the northeastern Australian margin: stable isotopic data from Leg 133, Sites 811 and 817, and Leg 21, Site 209. *In* McKenzie, J.A., Davies, P.J., Palmer-Julson, A., et al., *Proc. ODP, Sci. Results,* 133: College Station, TX (Ocean Drilling Program), 263–280.

Liu, K., Pigram, C.J., Paterson, L., and Kendall, C.G.St.C., 1998. Computer simulation of a Cainozoic carbonate platform, Marion Plateau, northeast Australia. *Spec. Publ. Int. Assoc. Sedimentol.,* 25:145–161.

Loeblich, A.R., and Tappan, H., 1988. *Foraminiferal Genera and Their Classification* (Vol. 2): New York (Van Nostrand Reinhold Co.).

Marshall, J.F., Tsuji, Y., Matsuda, H., Davies, P.J., Iryus, Y., Honda, N., and Satoh, Y., 1998. Quaternary and Tertiary subtropical carbonate platform development on the continental margin of southern Queensland, Australia. *Spec. Publ. Int. Assoc. Sedimentol.,* 25:163–195.

Martín, J.M., and Braga, J.C., 1993. Eocene to Pliocene coralline algae in the Queensland Plateau (northeastern Australia). *In* McKenzie, J.A., Davies, P.J., Palmer-Julson, A., et al., *Proc. ODP, Sci. Results,* 133: College Station, TX (Ocean Drilling Program), 67–74.

Martín, J.M., Braga, J.C., Konishi, K., and Pigram, C.J., 1993. A model for the development of rhodoliths on platforms influenced by storms: middle Miocene carbonates

of the Marion Plateau (northeastern Australia). *In* McKenzie, J.A., Davies, P.J., Palmer-Julson, A., et al., *Proc. ODP, Sci. Results,* 133: College Station, TX (Ocean Drilling Program), 455–460.

McKenzie, J.A., and Davies, P.J., 1993. Cenozoic evolution of carbonate platforms on the northeastern Australian margin: synthesis of Leg 133 drilling results. *In* McKenzie, J.A., Davies, P.J., Palmer-Julson, A., et al., *Proc. ODP, Sci. Results,* 133: College Station, TX (Ocean Drilling Program), 763–770.

Nebelsick, J.H., 1992. Components analysis of sediment composition in early Miocene temperate carbonate from the Austrian Paratethys. *Palaeogeogr., Palaeoclimatol., Palaeoecol.,* 91:59–69.

Noad, J., 2001. The Gomantong limestone of eastern Boreneo: a sedimentological comparison with the near-contemporaneous Luconia Province. *Palaeogeogr., Palaeoclimatol., Palaeoecol.,* 175:273–302.

Pigram, C.J., 1993. Carbonate platform growth, demise and sea level record: Marion Plateau, northeast Australia [Ph.D. dissert.]. Australian National Univ., Canberra.

Pigram, C.J., Davies, P.J., Feary, D.A., and Symonds, P.A., 1992. Absolute magnitude of the second-order middle to late Miocene sea-level fall, Marion Plateau, northeast Australia. *Geology,* 20:858–862.

Pomar, L., 2001. Ecological control of sedimentary accommodation: evolution from a carbonate ramp to rimmed shelf, upper Miocene, Balearic Islands. *Palaeogeogr., Palaeoclimatol., Palaeoecol.,* 175:249–272.

Pomar, L., Ward, W.C., and Green, D.G., 1996. Upper Miocene reef complex of the Llucmajor area, Mallorca, Spain. *In* Franseen, E.K., Esteban, M., Ward, W.C., and Rouchy, J.-M. (Eds.), *Models for Carbonate Stratigraphy from Miocene Reef Complexes of Mediterranean Regions*. Concepts Sedimentol. Paleontol., 5:191–225.

Robertson, A.H.F., 1998. Miocene shallow-water carbonates on the Eratosthenes Seamount, easternmost Mediterranean Sea. *In* Robertson, A.H.F., Emeis, K.-C., Richter, C., and Camerlenghi, A. (Eds.), *Proc. ODP, Sci. Results,* 160: College Station, TX (Ocean Drilling Program), 419–436.

Saint Martin, J.-P., André, J.-P., Müller, J., and Lapointe, P., 1997. Géométrie de la plate-forme carbonatée d'âge Messinien de Malte: mise en évidence de l'élévation du plan d'eau méditerranéen au cours du Messinien. *C. R. Acad. Sci., Ser. IIa: Sci. Terre Planetes,* 324:729–736.

Shipboard Scientific Party, 2002a. Leg 194 summary. *In* Isern, A.R., Anselmetti, F.S., Blum, P., et al., *Proc. ODP, Init. Repts.,* 194: College Station TX (Ocean Drilling Program), 1–88.

Shipboard Scientific Party, 2002b. Sites 1196 and 1199. *In* Isern, A.R., Anselmetti, F.S., Blum, P., et al., *Proc. ODP, Init. Repts.,* 194, 1–159 [CD-ROM]. Available from: Ocean Drilling Program, Texas A&M University, College Station TX 77845-9547, USA.

Sokal, R.R., and Rohlf, F.J., 2003. *Biometry: The Principles and Practice of Statistics in Biological Research:* New York (W.H. Freeman).

Vaughan, T.W., and Wells, J.W., 1943. Revision of the suborders, families and genera of the Scleractinia. *Geol. Soc. Am.,* 44:1–363.

Veron, J.E.N., 2000. *Corals of the World:* Townsville, M.C. (Australian Inst. Mar. Sci.).

Wells, J.W., 1956. Part F. Scleractinia. *In* Moore, R.C. (Ed.), *Treatise on Invertebrate Paleontology:* New York (Geol. Soc. Am.), F328–F444.

Figure F1. Location maps of ODP Leg 194 Sites 1196 and 1199 and Leg 133 sites with multichannel seismic lines (from Shipboard Scientific Party, 2002a, modified).

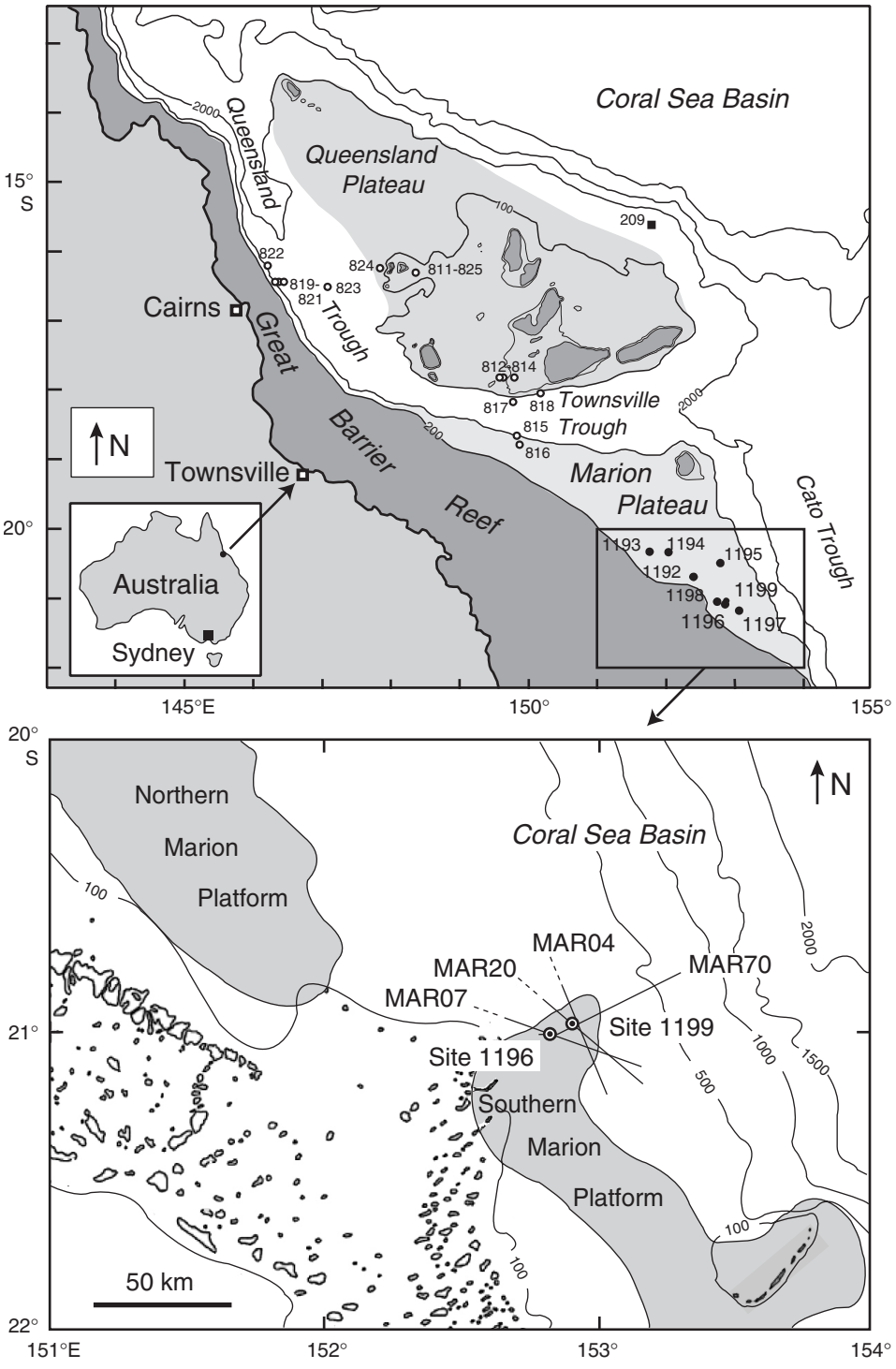

Figure F2. Seismic transect of the Southern Marion Plateau showing the position of Sites 1196 and 1199 and their respective lithostratigraphic units (Shipboard Scientific Party, 2002a). MS = megasequence.

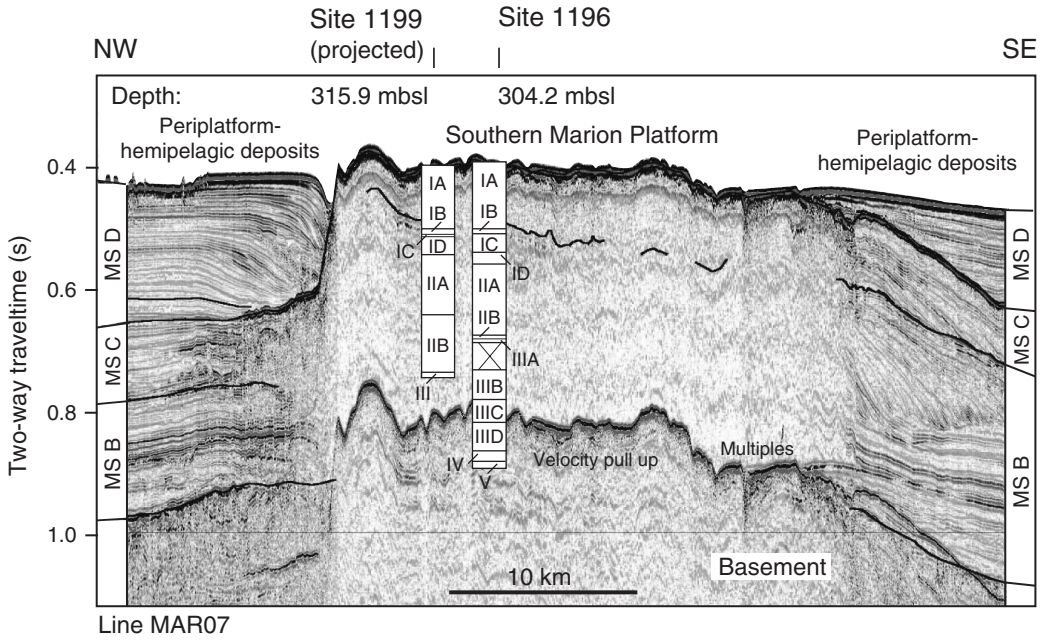

Figure F3. Schematic diagram representing the lithostratigraphy and the architecture of the SMP (figure F15E in Shipboard Scientific Party, 2002a). MS = megasequence.

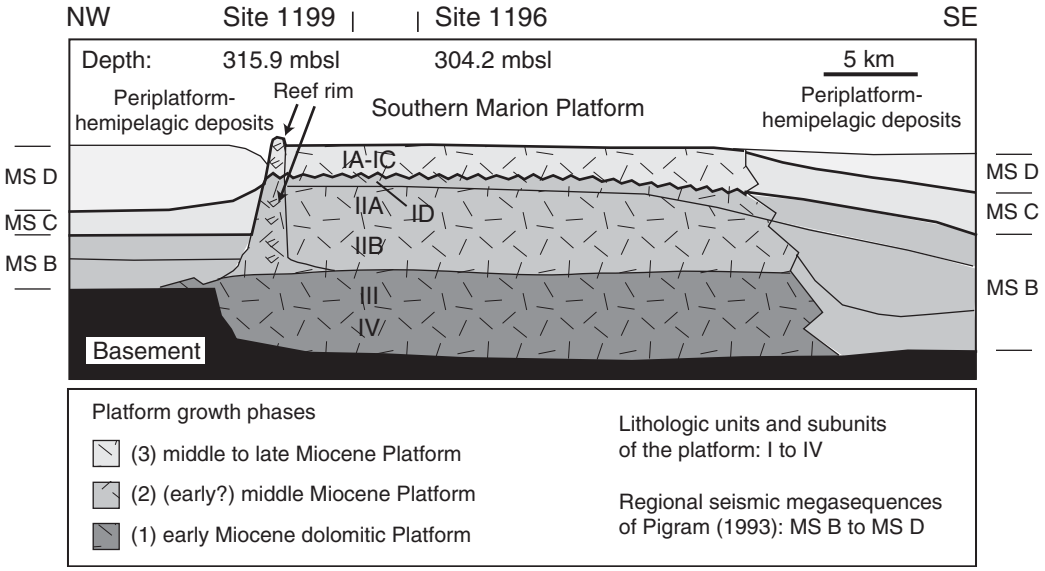

Figure F4. Microfacies matrix with percentage values of bioclasts and ascendant cluster analysis dendrogram. Aggl. = agglutinated.

Unit	Hole, core, section, interval (cm)	Algae			Invertebrates						Small benthic foraminifers				Larger benthic foraminifers											Planktonic foraminifers	Microfacies
											Aggl.	Hyaline			Porcellaneous			Hyaline									
																				Nummulitids							
		Red algae	Geniculate red algae	Green algae (*Halimeda*)	Corals	Echinoderms	Bivalves	Gastropods	Serpulids	Bryozoans	Small agglutinated foram.	Rotaliids	Small hyaline foram.	Miliolids	*Austrotrillina*	Soritids	Alveolinids	Hyaline encrusting foram.	*Amphistegina*	*Operculina*	*Operculinella*	*Cyclolypeus*	*Lepidocyclina*	*Miogypsina*		
	194-	RAL	GRA	HAL	COR	ECH	BIV	GAS	SER	BRY	SAF	ROT	SHF	MIL	AUS	SOR	ALV	HEF	AMP	OPE	OPA	CYC	LEP	MIO	PLF	
IA	1199A-13R-3, 115-119	66		4	15	9											2			4							
IB	1196B-17Z-1 , 54-57	78.5				19.5					1			1													F: Red algae-echinoderms
IIB	1199A-39R-1, 56-60	81				15								1			3										
IA	1199A-9R-4, 12-16	76				20													4								
	1199A-1R-1, 32-34	99.3				0.7																					
	1199A-1R-1, 3-6	93.5				5.4	0.4											0.7									
ID	1199A-17R-1, 23-26	80		2		18																					
IIB	1199A-35R-1, 13-17	72				28																					
ID	1199A-18R-3, 21-26	86				14																					
	1196A-18R-3, 75-78	86				14																					
IB	1199A-14R-1, 137-142	93.7				6.3																					
	1196A-14R-1, 42-46	93				7																					
IA	1199A-12R-5, 93-95	88	4			8																					
	1199A-11R-1, 16-20	87.9				7.8	0.5												1.2			1.2	1.4				
IIA	1196A-33R-1, 48-53	26.3	3.7	0.7	40.3	5.7	5.7	1	0.3	2.3	0.7	1	0.4	4.7	4.6	1			1							0.7	
IA	1199A-5R-2, 127-131	59.4		22.1	5.1	1.1	0.4	2.1		1.1								0.4	7.1							1.4	B: Corals
IC	1196A-15R-1, 0-3	17.8	1.6	24.1	30.8	1.3	1.3	1.1	1.3	0.8	0.3		0.6	1.6				12.3			0.8					4.3	
IIA	1196A-34R-1, 96-99		2.8			26.8	9.5	1.4	4.1	4.1	1.4	1.4	1.4	33.4						4.1						9.4	
	1196A-20R-1, 45-47					16.4	7.1	7.1		3.1	6.3	3.1	13.1	7.1		23.1										13.7	
	1199A-19R-1, 0-4	13.6				20.3	9.6		4.3	12.3	19			8.3		1.6										11	
ID	1199A-16R-3, 40-44	67	2	6		12	1			1						3			8								
IB	1196B-20Z-1, 16-20	82.7	0.3	7.3		6			1		0.7		0.3				1		0.7								
IIB	1199A-40R-1, 27-31	45.3	1	38.3		5.3	0.7	0.3		1	1		1.3	1.3	1		0.7		0.3	0.7						1.7	
	1196A-35R-1, 1-5	29.7	7.4	16		16	3	5.4	0.7	1	2		5	6.7	1				1.4	0.4			1.4	0.4	2.7	A: Porcellaneous foraminifers
	1199A-31R-1, 0-3	62.7	2.3	7		11.7	1.7	3		0.3	0.3	0.3		2.7	0.7	2		0.3	1.3	1			0.7			2	
	1196A-32R-1, 11-14	28.3	4.3			23.3	2.3	1.3		16.3	1.2	4.3	1.2	7.3	1.3	1.3	5.3		1.3							1.3	
	1196B-46Z-1, 14-17	28	0.4			24	5.7	0.4		13.4	2.7	0.4	3.3	6.7	5	1	1.7	2.4	1.4	1						2.7	
IIA	1196A-25R-1, 50-52	30.3	9.7			33	1.3		0.3	7.4	1.7	1	2	5.4	1.4	0.7	0.4		1.7	1.7			0.7	0.4	1	
	1196A-27R-1, 7-10	20	8.3	0.7		16	7.3		1	6.3	1.3		1	7.7	17.7	6.3	1.3	1	2.3							1.7	
	1196A-33R-2, 57-60	20.3	10.3	3		9.3	7.7	9	3.7	0.7	1.3	0.3	1	9.7	9	5.7	4.3	0.7	0.7	1						2.3	
	1196A-24R-1, 13-17	13.4	2.8			24.1	5.4	1.8	2.4	13.8	2.8	0.4	2.8	10.8	1.8	5.4	4.1		0.8	2.8			0.4	0.4	4.1	
	1196B-33Z-1, 3-5	56				24				3	2		4	1	2			3			4					1	
ID	1199A-16R-4, 91-96	78		9		10			3										2.3				11.3				
IA	1199A-10R-3, 58-60	40.7		41	0.7	2.7		0.3			1								1.4				0.7		0.4	E: *Halimeda-Lepidocyclina*
	1199A-4R-6, 138-140	64.4		31.7			0.7	0.7											0.8	0.8			5.8			
	1196B-14Z-1, 68-73	81.1		3.1		7.4	0.8			0.4																	
	1196A-13R-2, 38-41	82.3	2.3	2.7		7.3								0.3					0.3		0.7		5				
	1196A-11R-1, 24-28	73.3	4.3	13		3				0.7													4.7				
	1196A-10R-1, 8-12	82	3.7	1		1.7												7.7	1	1			2				
IIB	1199A-33R-1, 11-13	45.3	2.3	21.3		20.3				2.7	0.7	0.3		0.7					0.7		1		1.7	2.7	0.3	C: *Miogypsina-Lepidocyclina*
	1199A-34R-1, 28-31	71.3		0.3		14.4				1.3	1.3	0.3					0.7		5		1.3		2.7	1.3		
	1199A-39R-1, 91-94	68.7	1.3	0.3		6.7				1		0.7		1			1.7	3	1.3	1			7	6.3		
	1199A-40R-1, 9-13	58.7	1.7	0.7		7			4		1			1		0.7	2.7		8	1			1.3	11.7	0.7	
	1199A-41R-1, 19-22	32.4	3	6.7		13.7	2			8	3	1.4	1.4			0.7		5.7	2		0.4	1	7.7	7.7	3	
	1199A-37R-1, 2-6	49.7	1.3	15.7		5.3	4.3			4						0.3			2			0.3	13.3	2.7	1	
	1199A-42R-1, 83-85	54.3	1	1.3		7.7	0.7			4.7								2	6.7	1.7	0.3	2.7	11.7	5.3		
IC	1196A-16R-1, 25-27	68.4		8.4		4.1	0.4	1	0.4	1.7				0.4				6	0.7	1	0.4	0.7	2	3.1	1.4		
IA	1199A-2R-3, 20-23	54.8		30.8		4.8					0.8								2.8		1.8	1.8	2.5			D: *Halimeda*-Nummulitids-*Amphistegina*
	1199A-6R-3, 69-72	63.3		11.7		4												3	16.3				1.7			
	1196B-4R-1, 28-30	33	0.3	14.3		5	0.7			5	0.7	0.3	0.7					6.3	15.7	1.3	0.3	5.3	3.3		7.7		
	1196A-5R-1, 70-72	54.4		12.4		5.4					0.4							9.1	13.1	0.4	1.4	0.7	1.1		1.7		
ID	1196A-18R-2, 15-18	70.1	3.1	16.4		4.1		1.4						1.1				0.4	1.8		1.4						
IA	1199A-3R-1, 77-81	78.7	0.7	7.7	3	1.3													3.7	0.7	3.3	1					
	1196A-7R-1, 106-109	67.4	6.1	1.4		10.8			0.8	0.4								0.8	3.8		5.8	1.1			1.8		
	1196A-5R-2, 74-77	47.7	4.7	18.4	1.7	1.4		0.7										4.1	9.1		6.4	4.4			1.4		
	1196B-1R-3, 1-6	29.4		29.4	5.1	4.4	1.6	0.8	0.4	0.6	0.8			1.3			1.2	1.1	8.4	1.8	4	1			8.8		
IIA	1199A-20R-1, 17-22	20.1		3.1	2.7	18.1	4.1		1.7	1.7	3.1	0.4	0.7	2.1	1.4	11.7	2.1	15.7	4.1		1.7	1.4	1.1	2.7	0.4		
	1196A-21R-1, 119-121	26	2	3	4.7	16	5.3	1.7	2	0.3	3	1.3	3.3	6.7		0.7	6	1	2	2	3	1.7	3.7	2.3	2.3		
IA	1196A-1R-1, 35-40	76.4	1.1	0.4	4.1	4.8		0.4		0.8	0.4	0.8		2				3.1	3		2.4	0.8					

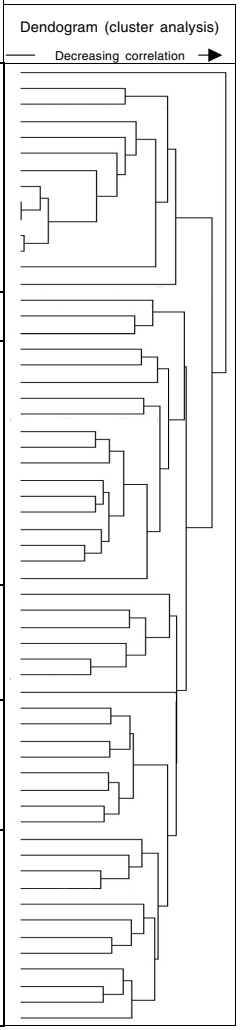

Figure F5. Lithostratigraphic columns with biosedimentological data, microfacies, and environment evolution. **A.** Site 1196. Cor. = coral, infl. = influence, PF = platform, Exp. = exposure, limest. = limestone. (Continued on next page.)

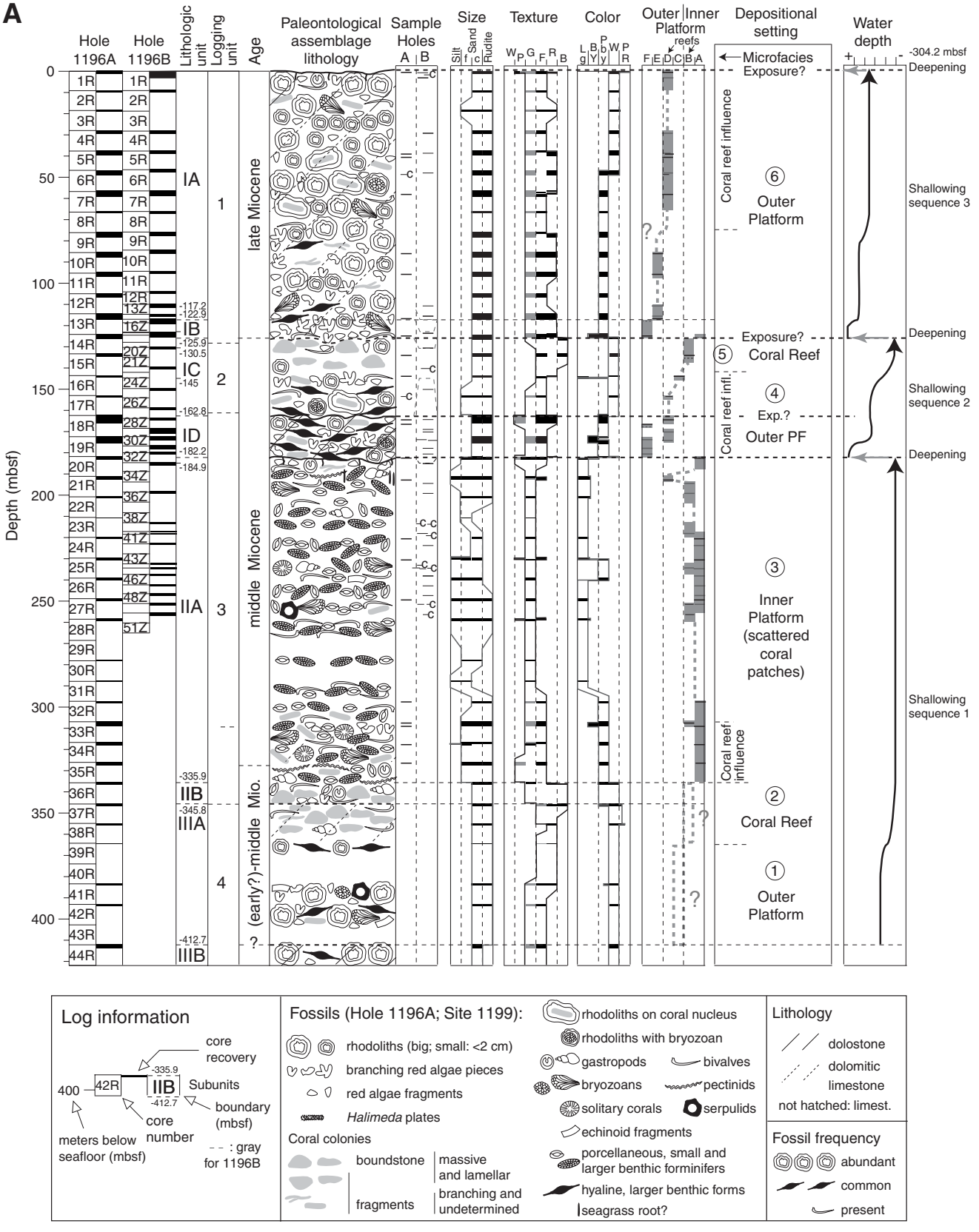

Figure F5 (continued). B. Site 1199.

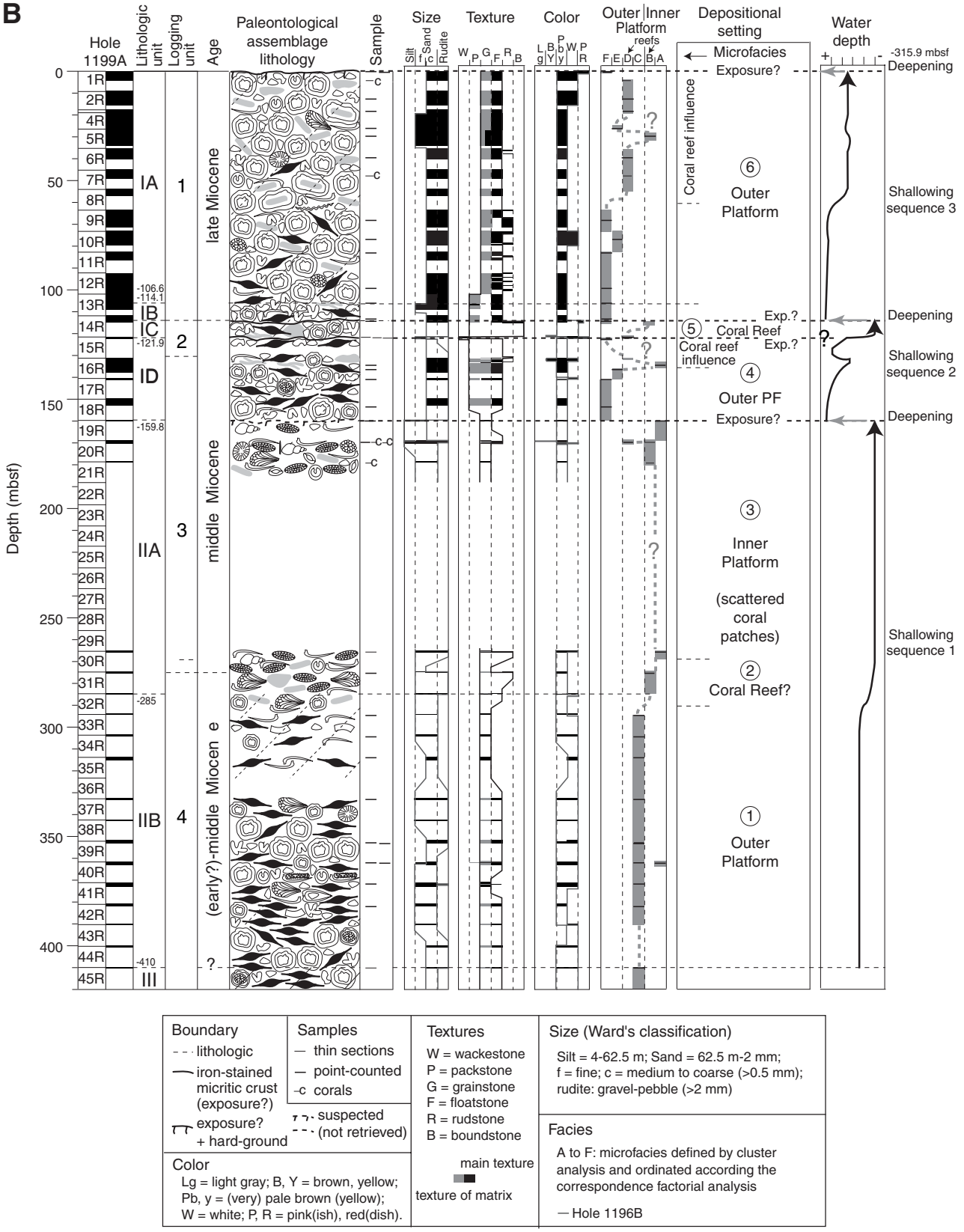

Figure F6. Correlation of uranium and resistivity logs of Holes 1196A and 1199A (figure F70 in Shipboard Scientific Party, 2002b).

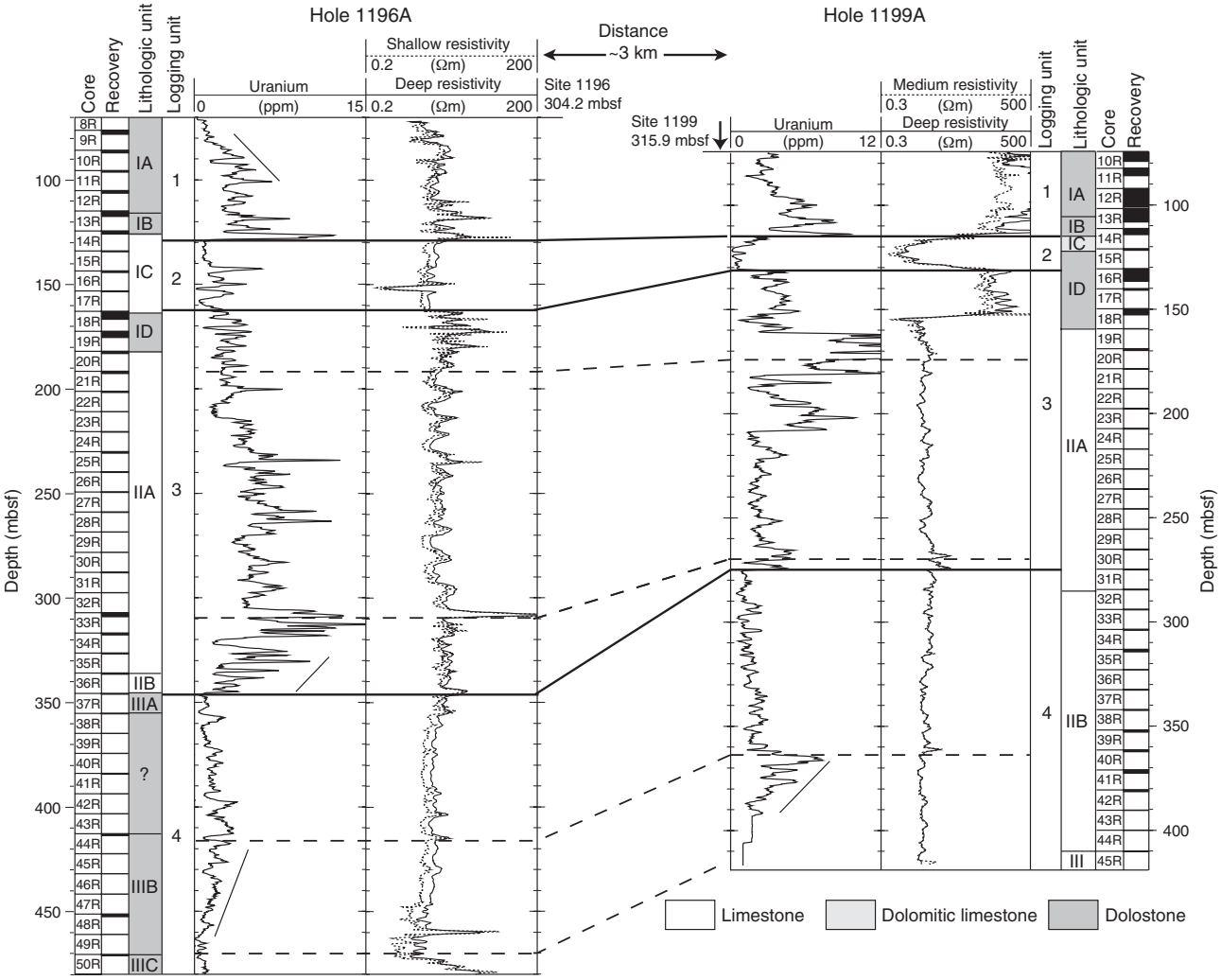

Figure F7. Correspondence factor analysis (CFA) planes of axes 1-2 and 1-3 with microfacies and environmental interpretation. The variance of each axis is given in percentage. Circled groups of samples = main microfacies (A–F) defined by the cluster analysis. See Table T2, p. 37, for variable definitions. Variables in bold with arrow and absolute contribution in percentage = significant variables according to specified factorial axes.

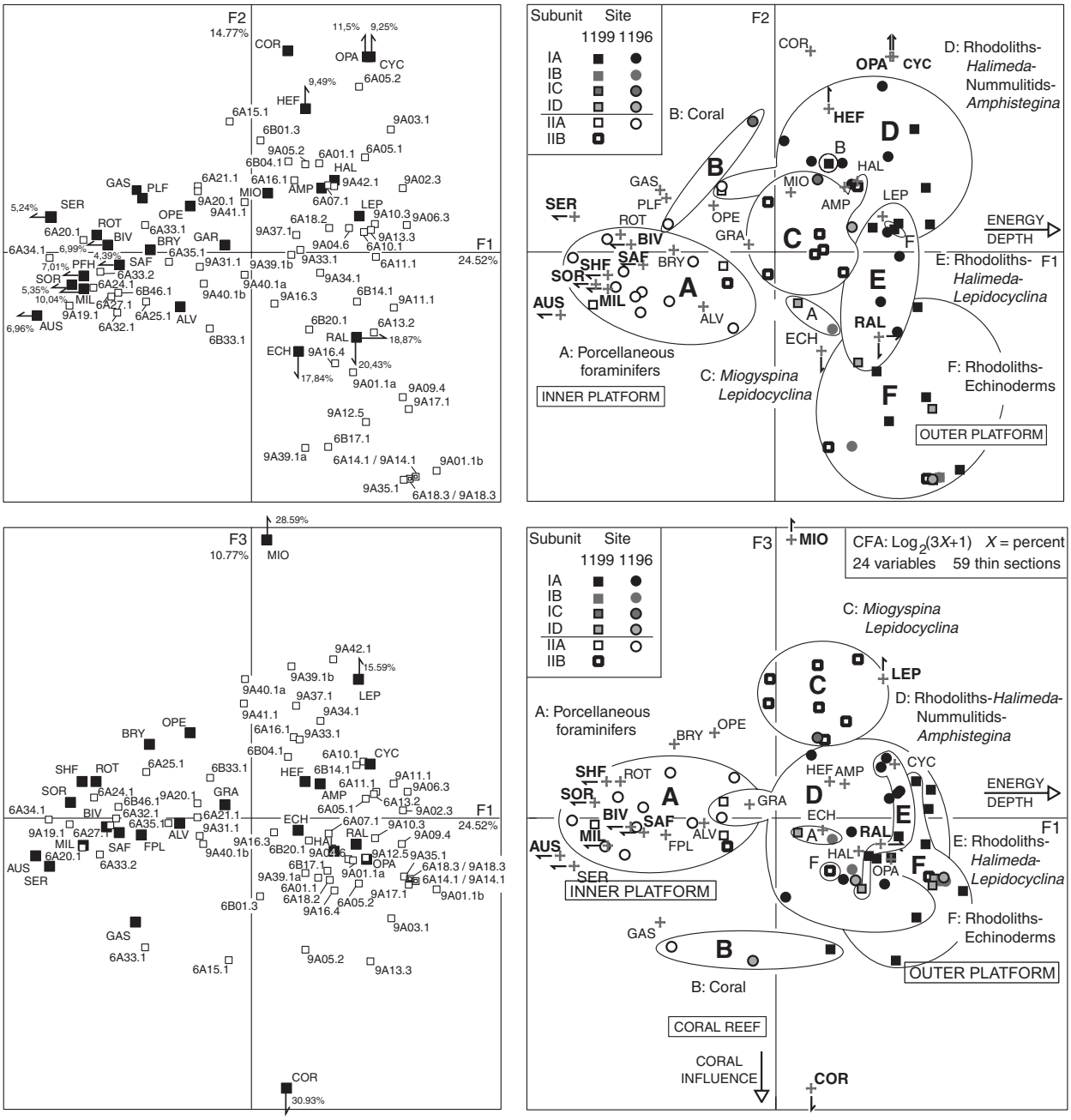

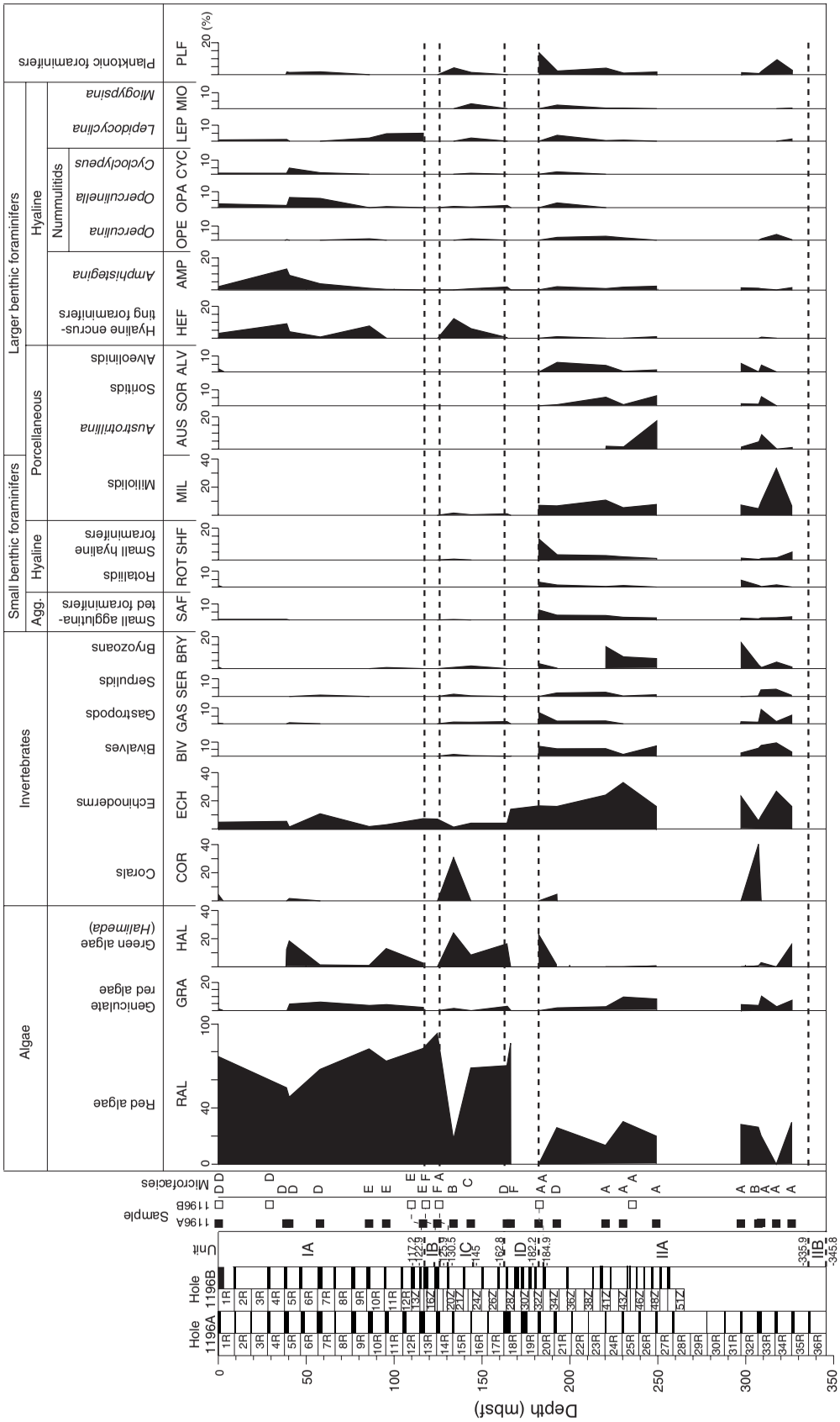

Figure F8. Frequency of microfacies biogenic components vs. Site 1196 lithostratigraphic column. Agg. = agglutinated.

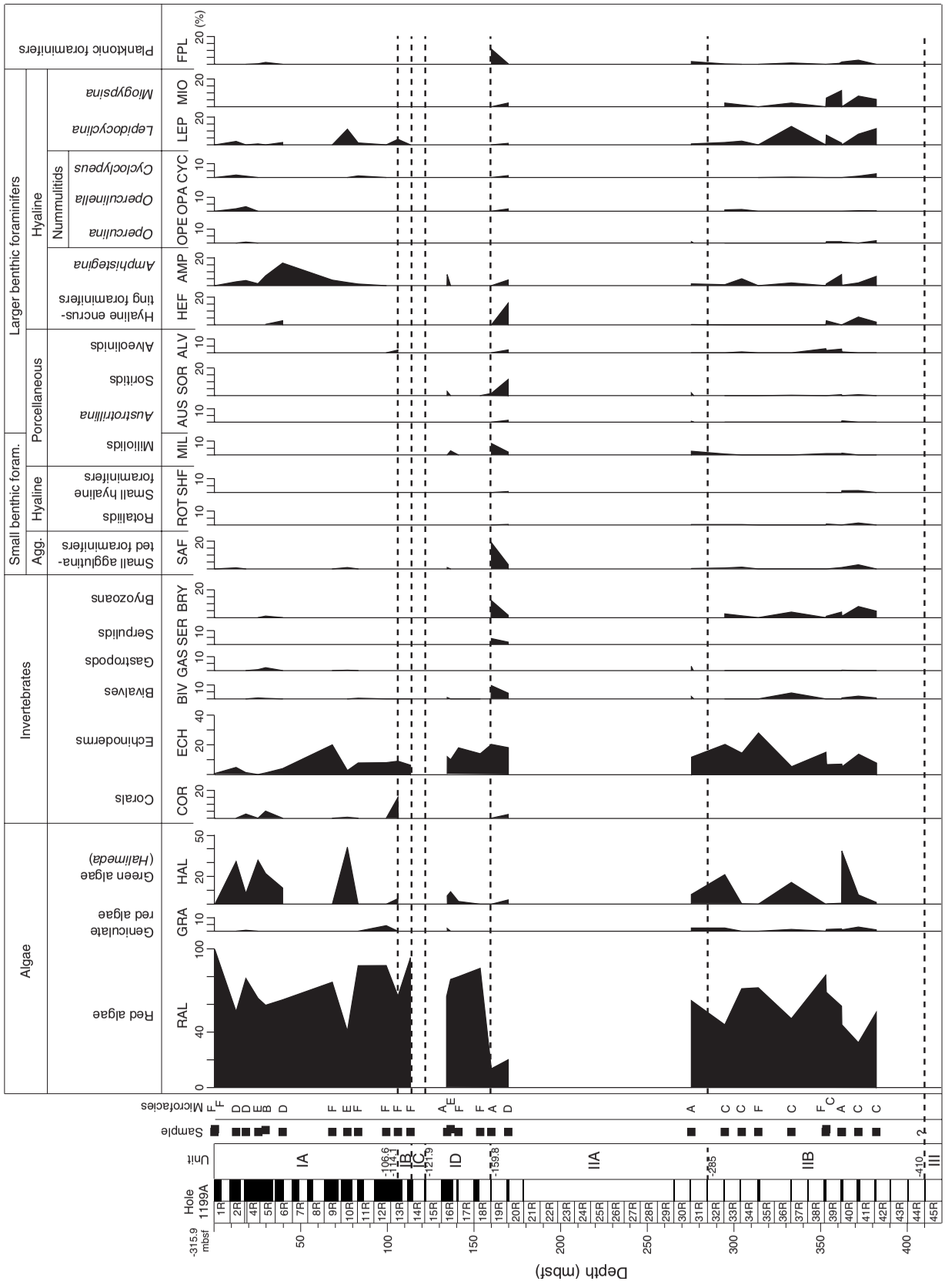

Figure F9. Frequency of microfacies biogenic components vs. Site 1199 lithostratigraphic column. foram. = foraminifer, Agg. = agglutinated.

Figure F10. Traces of well-defined seismic reflections of Line MAR07 at Site 1196 with corresponding lithostratigraphic units (seismic data from fig. F74 in Shipboard Scientific Party, 2002b).

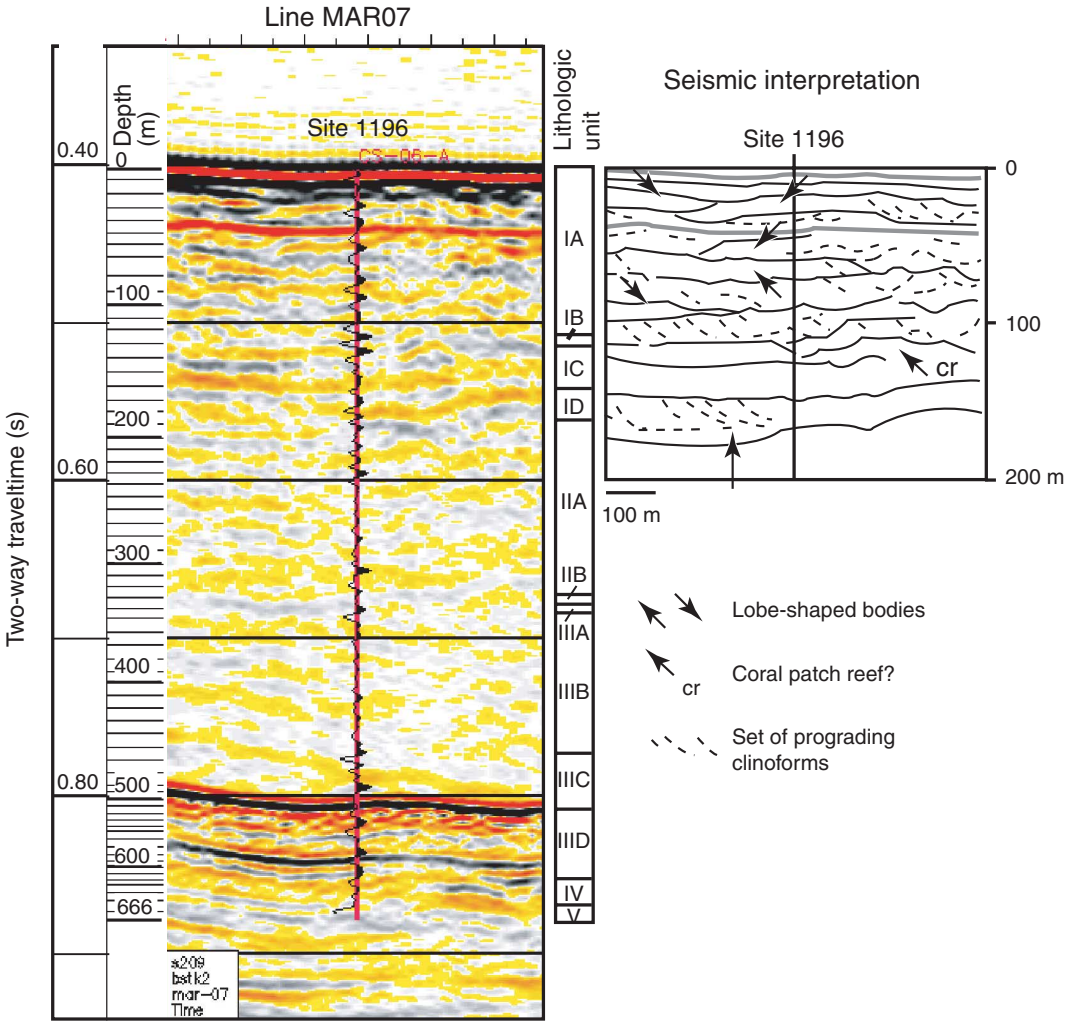

Figure F11. Reconstructions of the depositional environments at the scale of sedimentary bodies (1 km) from the Southern Marion Platform.

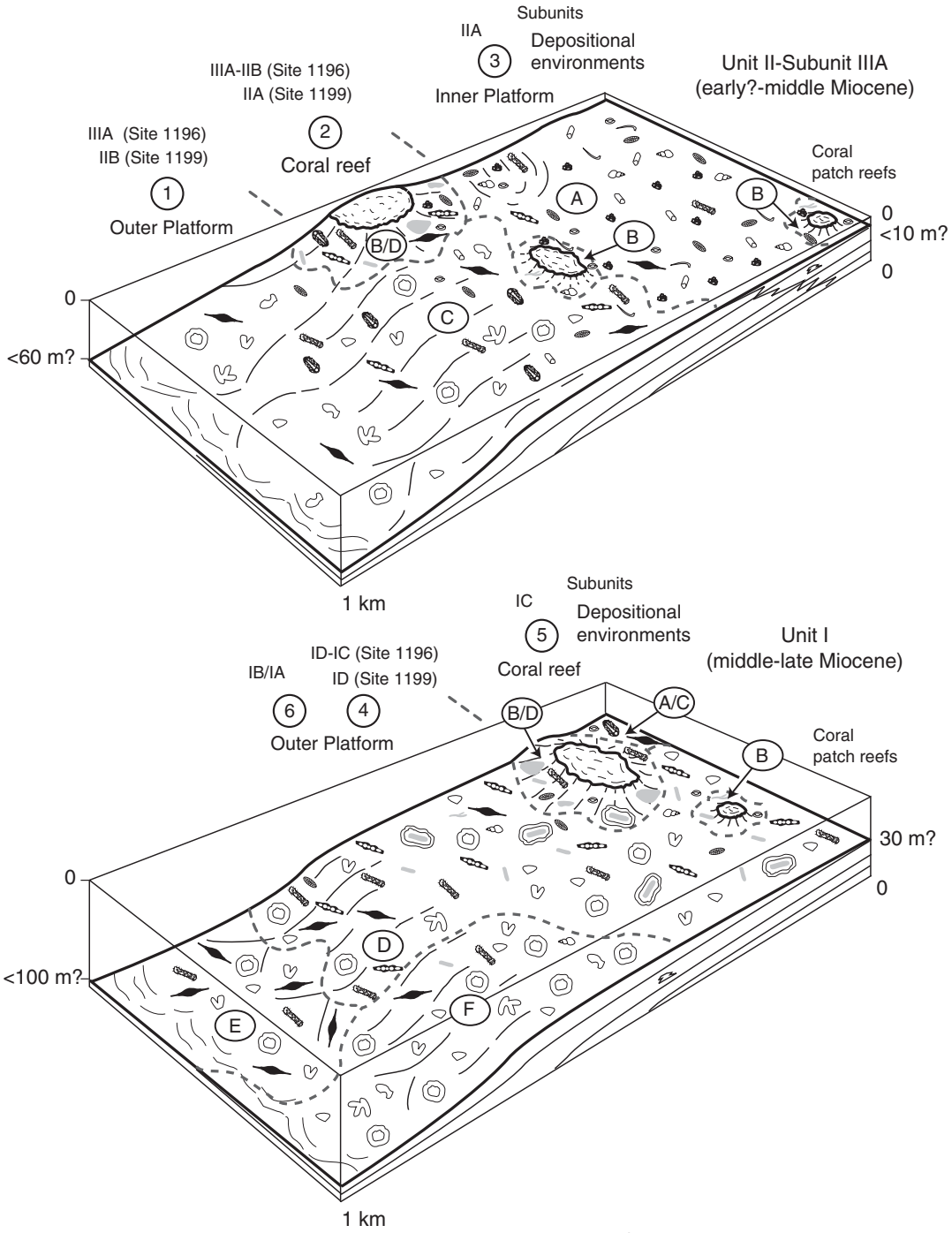

Table T1. List of coral taxa with their ecological significance (Sites 1196 and 1199).

Unit	Core, section, interval (cm)	Coral taxa	Ecology	
IA	194-1196A-			
	6R-1, 105–107	*Acanthophyllia* cf. *deshayesiana* (Michelin, 1850)	Solitary (within reef)	Carbonate rich and warm water
	194-1196B-			
	1R-2, 8–12	*Lithophyllon* cf. *mokai* Hoeksma, 1989	Secondary framebuilders	High energy resistant
	194-1199A-			
	1R-3, 125–129	cf. *Favites pauciseptata* Gerth, 1923	Secondary framebuilders	High energy resistant
	7R-2, 121–125	*Stylophora cambridgiensis* Wells, 1934	Secondary framebuilders	Low energy, well oxygenated
IB	194-1196A-			
	17R-1, 21–25	*Stylophora depauperata* (Reuss, 1867)	Secondary framebuilders	Low energy, well oxygenated
IC	194-1196B-			
	22Z-1, 38–44	*Alveopora polyacantha* Reuss, 1867	Secondary framebuilders	Low energy, well oxygenated
		Stylophora subseriata (Ehrenberg, 1834)	Secondary framebuilders	Low energy, well oxygenated
IIA	39Z-1, 24–29	*Trematotrochus* sp.	Solitary	Ubiquitous
	39Z-1, 46–49	*Antiguastraea* aff. *alveolaris* (Catullo, 1856)	Secondary framebuilders	Low energy, well oxygenated
	41Z-1, 16–19	*Stylophora* cf. *cambridgiensis* Wells, 1934	Secondary framebuilders	Low energy, well oxygenated
	194-1199A-			
	20R-1, 40–50	*Pavona (Hydnophoseris)* sp.	Secondary framebuilders	Low energy, well oxygenated
	21R-1, 6–8	*Stylophora granulata* Duncan and Wall, 1864	Secondary framebuilders	Low energy, well oxygenated

Table T2. Summary of the correspondence factor analysis.

Biological variables			AC axes			RC axes		
Number	Acronym		F1	F2	F3	F1	F2	F3
1	RAL	Red algae	**1887**	**2043**	272	**5553**	**3620**	352
2	GRA	Geniculate red algae	27	3	15	182	15	45
3	HEF	Hyaline encrusting foraminifers	80	**949**	81	394	**2809**	175
4	HAL	*Halimeda*	478	619	179	2059	1606	339
5	COR	Corals	23	1272	**3093**	70	2273	**4028**
6	SER	Serpulids	**524**	27	69	**4010**	128	232
7	BIV	Bivalves	**699**	3	5	**6100**	19	20
8	GAS	Gastropods	257	126	479	1857	546	1515
9	ECH	Echinoderms	244	**1784**	39	1495	**6562**	104
10	BRY	Bryozoans	413	0	498	3836	3	2028
11	PLF	Planktonic foraminifers	414	174	20	3796	964	83
12	SAF	Small agglutinated foraminifers	**439**	6	11	**4339**	37	50
13	SHF	Small hyaline foraminifers	**701**	21	75	**5310**	97	251
14	AMP	*Amphistegina*	244	350	138	1789	1547	443
15	ROT	Rotaliids	296	6	36	2774	36	148
16	MIL	Miliolids	**1004**	74	57	**6642**	297	168
17	AUS	Austrotrillina	**696**	96	48	**3894**	326	119
18	SOR	Soritids	**535**	27	9	**3560**	109	26
19	ALV	Alveolinids	101	95	1	569	321	3
20	OPE	*Operculina*	63	62	280	552	326	1069
21	OPA	*Operculinella*	242	**1150**	70	1277	**3642**	162
22	CYC	*Cycloclypeus*	202	**925**	97	1195	**3292**	251
23	LEP	*Lepidocyclina*	413	80	**1559**	1886	221	**3124**
24	MIO	*Miogypsina*	4	95	**2859**	19	261	**5718**

Notes: AC = absolute contributions in 1/10,000. RC = relative contributions (r^2 × 10,000). Bold = the absolute and relative contributions of discriminate variables to axis. Eigenvalue and percentage of total inertia explained by the individual factor axes, cumulative percentage, and percentage of variables' contributions to each axis are listed. F1: eigenvalue = 0.26503, relative inertia = 24.52%, cumulative = 24.52%; F2: eigenvalue = 0.15961, relative inertia = 14.77%, cumulative = 39.29%; F3: eigenvalue = 0.11637, relative inertia = 10.77%, cumulative = 50.06%; F4: eigenvalue = 0.08016, relative inertia = 7.42%, cumulative = 57.48%.

Plate P1. 1. Transverse section of *Austrotrillina howchini* (Schlumberger), 10× (Sample 194-1196A-35R-1, 13–17 cm). **2.** Axial section of *Flosculinella bontangensis* (Rutten), 5× (Sample 194-1196B-46Z-1, 14–17 cm). **3.** Floatstone-grainstone with *Miogypsina* sp. and small hyaline foraminifers, 2.5× (Sample 194-1199A-41R-1, 19–22 cm). **4.** *Lepidocyclina* sp., geniculate red algae, and echinoid spine, 2.5× (Sample 194-1199A-41R-1, 19–22 cm). **5.** Floatstone-poor packstone with mudstone internal sediment and micritized bioclasts including *Operculinella* sp. and Rotaliids, 2.5× (Sample 194-1196A-5R-2, 74–77 cm). **6.** Floatstone-grainstone with *Cycloclypeus* sp., rounded fragments of red algae, and *Halimeda* plate, 2.5× (Sample 194-1196A-5R-2, 74–77 cm).

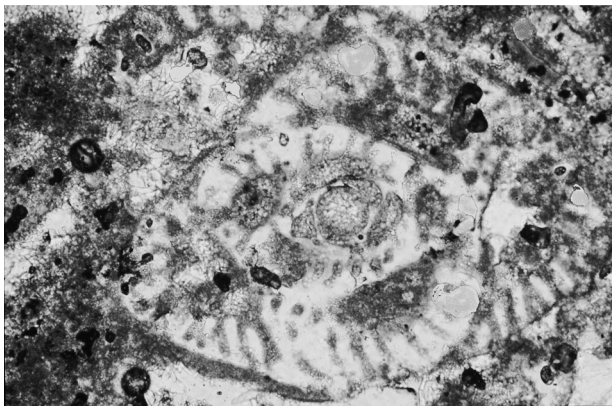
1

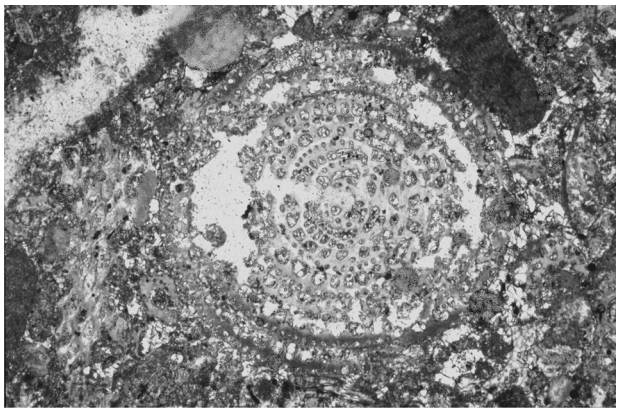
2

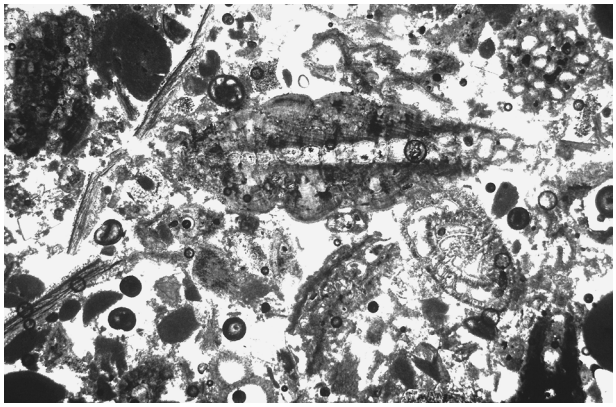
3

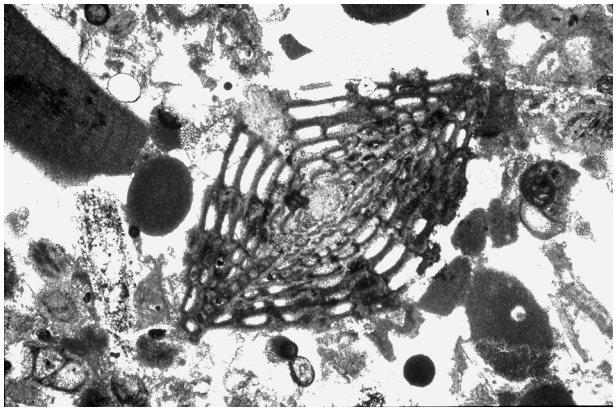
4

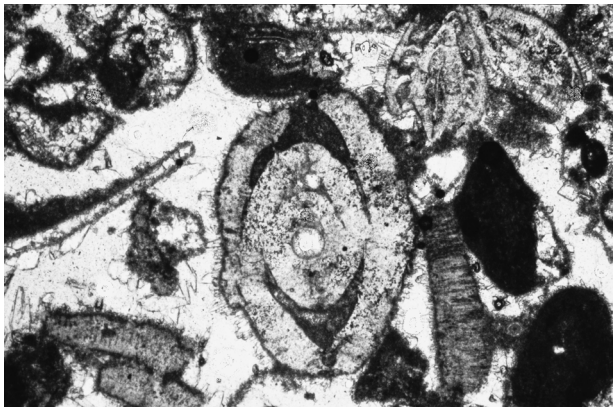
5


6